Massachusetts Institute of Technology
Department of Civil Engineering
Constructed Facilities Division
Cambridge, Massachusetts 02139

DYNAMIC BEHAVIOR OF EMBEDDED FOUNDATIONS

by

F. Elsabee

and

J. P. Morray

Supervised by

José M. Roesset

September 1977

Sponsored by the National Science Foundation
Division of Advanced Environmental Research and Technology

NSF-RANN Grant No. AEN-7417835

Publication No. R77-33 Order No. 578

ABSTRACT

The three-step or substructure approach to the solution of soil-structure interaction problems becomes particularly convenient when analytical or semi-analytical solutions can be used for each one of the first two steps: determination of the seismic motions at the base of a massless foundation and computation of the dynamic stiffness matrix of the foundation. Unfortunately these solutions are only available at present for surface foundations, while most massive structures, such as nuclear power plants, will always have some degree of embedment.

In this work the results of a series of parametric studies using a three-dimensional, cylindrical finite element formulation with consistent lateral boundaries are presented. From these results approximate rules are suggested to derive:

— the translational and rotational components of motion at the base of a rigid, massless embedded foundation from the specified seismic input at the free surface of the soil in the free field. The importance of the rotational component is illustrated and its dependence on the flexibility of the sidewalls, the actual conditions of the backfill, and the possible loss of contact between the sidewalls and the soil is discussed.

— the dynamic stiffness matrix of an embedded rigid and massless foundation from the results already available for a surface foundation.

The degree of approximation provided by these rules is illustrated for a specific and particularly unfavorable case. It is concluded that these simplified rules can be used at least for preliminary analyses in order to evaluate the importance of the interaction effect and the relative influence of various parameters.

PREFACE

The work described in this report represents a summary of the theses of F. Elsabee and J. P. Morray, presented to the Civil Engineering Department at M.I.T. in partial fulfillment of the requirements for the degree of Master of Science. Messrs. Elsabee and Morray were graduate students at M.I.T. under the Engineering Residence program with Stone and Webster Engineering Corporation. Their work at M.I.T. was supervised by Professor J. M. Roesset initially and by Professor Robert V. Whitman later. Their work at Stone and Webster was supervised by Dr. E. Kausel. Additional results included in this report were obtained by Dr. Kausel and Professor Roesset.

The research reported was made possible in part through Grant AEN-7417835 from the National Science Foundation, Division of Advanced Environmental Research and Technology.

This is the fourth of a series of reports published under this grant. The other three are:

1. Research Report R76-8 by Mohammed M. Ettouney, "Transmitting Boundaries: A Comparison," January 1976.

2. Research Report R76-9 by Mohammed M. Ettouney, "Nonlinear Soil Behavior in Soil Structure Interaction Analysis," February 1976.

3. Research Report R77-30 by J. J. Gonzalez, "Dynamic Interaction between Adjacent Structures," September 1977.

DYNAMIC BEHAVIOR OF EMBEDDED FOUNDATIONS

INTRODUCTION

The effect of the flexibility of the underlying soil on the dynamic response of structures has been a subject of considerable interest and research in recent years, particularly in relation to the seismic analysis of massive structures such as nuclear power plants.

Two general approaches are used at present for the solution of soil-structure interaction problems:

— A one-step or direct approach, in which the soil and the structure are modelled and analyzed together, using finite elements (or finite differences) and linear members. The model of the structure is normally a very simplified one, appropriate for the determination of the interaction effects (the motion at the base of the building or the accelerograms at various floor levels), but insufficient for the purpose of structural design. The input motion is applied at the base of the soil profile, requiring the use of a previous deconvolution if the design earthquake is specified at the free surface of the soil (as is normally the case). This procedure would have a definite theoretical advantage if a true three-dimensional model were used and nonlinear constitutive equations were utilized for the structure and especially the soil, with a step-by-step solution of the equations of motion in the time domain. The way it is commonly applied, with essentially a two-dimensional model of the soil and the use of an equivalent linearization technique to simulate nonlinear soil behavior, this advantage disappears.

— A three-step approach, also referred to as the substructure or spring method. In this case the first step is the determination of the seismic motion at the foundation level, considering a massless foundation. This step can be bypassed for a surface foundation if it is assumed that the seismic excitation consists of shear waves propagating vertically through the soil and the design earthquake is specified at the free surface of the deposit. It is necessary in all other cases. The second step is the determination of the dynamic stiffnesses of the foundation, complex functions of frequency (two, three or six stiffness functions if the foundation is assumed to be rigid and a complete dynamic stiffness matrix for a flexible foundation). The final step is the dynamic analysis of the structure resting on frequency-dependent "springs" as obtained in the second step and subject to the base motions computed in the first. This procedure implies the validity of superposition and is therefore restricted in rigor to linear analyses or studies in which nonlinearities are simulated through an equivalent linearization. It offers on the other hand considerably more flexibility in the way each step is handled, and it is particularly suited to parametric studies.

The three-step approach is particularly convenient when analytical or semi-analytical (simplified) solutions can be used for each one of the first two steps. These solutions exist now for horizontally stratified soil deposits and rigid surface foundations. The purpose of this work is to investigate the effect of embedment on the behavior of foundations and to derive simplified, approximate rules, to determine both the motions at the base of the foundation from the specified input at the free surface of the soil and the stiffnesses of an embedded foundation from those of a surface one. These rules could then be used at least for preliminary analyses in order to assess the importance of the interaction effects and the sensitivity of the results to variations in the basic parameters (characteristics of the input motion, soil properties, etc.).

For simplicity the majority of the studies are limited to the consideration of a rigid circular foundation embedded in a homogeneous soil stratum of finite depth (resting on much stiffer rock-like material which can be considered as rigid). It is assumed, furthermore, that the seismic motions are caused by vertically propagating shear waves (the usual assumption in present studies). It must be noticed, however, that these are not limitations of the three-step approach, but rather simplifications introduced here to limit the number of parameters. When dealing with a flexible foundation, the derivation of simplified formulae is nevertheless more difficult, because it is necessary to obtain both the motions and the equivalent forces at all contact points of the interface between the soil and the foundation and to determine a complete stiffness matrix with size equal to the product of the number of degrees of freedom at each node (2 or 3 depending on the model) by the number of contact nodes at the interface. A limited number of studies were, however, conducted considering flexible lateral sidewalls for the foundation and a soil deposit with modulus increasing with depth, in order to investigate the effect of these more realistic conditions.

FORMULATION

The solutions presented in this work were obtained with a three-dimensional axisymmetric finite element formulation. A layer of soil of finite depth resting on much stiffer, rock-like material was assumed, and the bottom boundary of the model was therefore considered rigid. The lateral boundaries were reproduced through a consistent boundary matrix developed by Waas (21) for the plane strain case and extended by Kausel (9) to the three-dimensional case. This transmitting boundary can be regarded as a virtual extension of the finite element mesh to infinity and has been shown to provide results in excellent agreement with analytical solutions even when placed directly at the edge of the foundation (3,9). It is important to notice that contrary to what has been sometimes reported (see 11 for instance) the use of this boundary matrix is not restricted to the solution of axisymmetric problems. For the situations studied here, the geometry of the problem must indeed be axisymmetric: thus the consideration of circular foundations. The loads or excitation may have, however, any distribution expanding them in a Fourier series along the circumference (the approach normally used for the solution of of shells of revolution under arbitrary loadings). For the study of the foundation stiffnesses, the term $n=0$ is to be used for vertical or torsional excitation, and the term $n=1$ for horizontal forces (swaying) or rocking moments (the two types of excitation studied here).

Consider a finite element discretization of the soil structure system as shown schematically in figure 3. Let K denote a dynamic stiffness matrix including inertia and damping terms for a steady state motion with frequency Ω, P represent forces and U absolute displacements. The following subscripts can be used:

- s for the nodes of the structure excluding the soil structure interface.
- b for the nodes of the structure along the interface.
- f for the nodes of the soil along the same interface.
- g for the nodes of the soil excluding the interface and the boundaries.
- r for the nodes along the bottom boundary of the soil.
- ℓ for the nodes along the lateral boundary.

Let finally L denote the consistent boundary matrix for the lateral boundary, U'_ℓ the displacements along this boundary in the free field, P'_ℓ the corresponding forces, and U_r the specified displacements at the bottom. Notice that U'_ℓ P'_ℓ can be obtained from an analytical (or numerical) solution of the wave propagation problem for any train of waves. This determination is particularly simple for a horizontally stratified soil deposit.

The equations of motion for the complete soil-structure system are:

$$\begin{bmatrix} K_{ss} & K_{sb} & 0 & 0 \\ K_{bs} & K_{bb}+K_{ff} & K_{fg} & K_{f\ell} \\ 0 & K_{gf} & K_{gg} & K_{g\ell} \\ 0 & K_{\ell f} & K_{\ell g} & K_{\ell\ell}+L \end{bmatrix} \begin{Bmatrix} U_s \\ U_b \\ U_g \\ U_\ell \end{Bmatrix} = \begin{Bmatrix} 0 \\ -K_{fr}\,U_r \\ -K_{gr}\,U_r \\ P'_\ell + LU'_\ell - K_{\ell r}\,U_r \end{Bmatrix}$$

where in general K_{fr} will be zero if there is more than one row of finite elements between the base of the structure and the bottom of the soil deposit.

This system of equations can be partitioned into two different ones;

for the structure

$$\begin{bmatrix} K_{ss} & K_{sb} \\ K_{bs} & K_{bb} \end{bmatrix} \begin{Bmatrix} U_s \\ U_b \end{Bmatrix} = \begin{Bmatrix} 0 \\ P_b \end{Bmatrix}$$

for the soil

$$\begin{bmatrix} K_{ff} & K_{fg} & K_{f\ell} \\ K_{gf} & K_{gg} & K_{g\ell} \\ K_{\ell f} & K_{\ell g} & K_{\ell\ell} + L \end{bmatrix} \begin{Bmatrix} U_b \\ U_g \\ U_\ell \end{Bmatrix} = \begin{Bmatrix} -P_b - K_{fr} U_r \\ -K_{gr} U_r \\ P'_\ell + LU'_\ell - K_{\ell r} U_r \end{Bmatrix}$$

where $P_b = - P_f$ are the forces between the structure and the soil at the interface and $U_b = U_f$ are the displacements of the contact nodes.

From this last set of equations it is possible to eliminate U_g, U_ℓ, writing

$$AU_f = AU_b = P_f - K_{fr} U_r - B = - P_b - K_{fr} U_r - B$$

or in general $$AU_b = - P_b - B \qquad \text{for } K_{fr} = 0.$$

In these expressions

$$A = K_{ff} - [K_{fg} \; K_{f\ell}] \begin{bmatrix} K_{gg} & K_{g\ell} \\ K_{\ell g} & K_{\ell\ell} + L \end{bmatrix}^{-1} \begin{bmatrix} K_{gf} \\ K_{\ell f} \end{bmatrix}$$

$$B = [K_{fg} \; K_{f\ell}] \begin{bmatrix} K_{gg} & K_{g\ell} \\ K_{\ell g} & K_{\ell\ell} + L \end{bmatrix}^{-1} \begin{Bmatrix} -K_{gr} U_r \\ P'_\ell + LU'_\ell - K_{\ell r} U_r \end{Bmatrix}$$

The equations for the structure can then be written as:

$$\begin{bmatrix} K_{ss} & K_{sb} \\ K_{bs} & K_{bb} + A \end{bmatrix} \begin{Bmatrix} U_s \\ U_b \end{Bmatrix} = - \begin{Bmatrix} 0 \\ B \end{Bmatrix}$$

A is the stiffness matrix of the foundation (soil-structure interface). It represents the forces at the nodes f of the soil system necessary to produce unit displacements of these same points when there is no seismic excitation ($U_r = B = 0$).

Defining, on the other hand

$$U_{bo} = - A^{-1}B \quad (\text{or} \quad -A^{-1}(K_{fr}\, U_r + B))$$

it can be seen that U_{bo} are the displacements of the nodes f of the soil system when there is no structure ($P_f = P_b = 0$) and the soil deposit with the excavation is subjected to the seismic input.

The equations of motion of the structure on elastic foundation can be finally written as

$$\begin{bmatrix} K_{ss} & K_{sb} \\ K_{bs} & K_{bb} + A \end{bmatrix} \begin{Bmatrix} U_s \\ U_b \end{Bmatrix} = \begin{Bmatrix} 0 \\ AU_{bo} \end{Bmatrix}$$

If it is assumed that the foundation is rigid, the displacements of the nodes at the interface U_f or U_b can be expressed in terms of the displacements of one point (the centroid of the base, for instance) by a relationship of the form

$$U_b = T^T\, U_c$$

where T^T is a rigid body transformation matrix.

The resultants at the same point of the forces at the interface nodes P_b are given by

$$P_c = TP_b$$

and the final equations of motion become

$$\begin{bmatrix} K_{ss} & K_{sb}\, T^T \\ TK_{bs} & TK_{bb}\, T^T + K_o \end{bmatrix} \begin{Bmatrix} U_s \\ U_c \end{Bmatrix} = \begin{Bmatrix} 0 \\ K_o U_{co} \end{Bmatrix}$$

with
$$K_o = TAT^T$$

and
$$K_o U_{co} = - TB$$

In this work a rigid foundation is assumed. The objective is to derive simplified expressions for the stiffness matrix K_o and the displacement vector U_{co}. For a seismic excitation causing only horizontal displacements in phase in the free field (shear waves propagating vertically through the soil deposit), the only motions induced in the foundation (at the center of its base) will be a horizontal translation and a rotation. In this case, the matrix K_o will be 2 x 2 and the vector U_{co} will have two components.

MOTION OF AN EMBEDDED FOUNDATION

For the case of SH or SV waves propagating vertically through the soil, the variation of motion with depth in the free field of a horizontally stratified deposit will be given by one-dimensional amplification theory. This theory is now well understood (16) and needs not be discussed in detail here. For a homogenous layer of soil, the motion at any depth z will be given by

$$u = A(e^{ipz} + e^{-ipz})\ e^{i\Omega t}$$

with
$$p^2 = \frac{\rho\Omega^2}{G(1+2iD)}$$

ρ is the mass density of the soil, G its shear modulus, D the amount of internal soil damping of a hysteretic nature (frequency independent) and Ω is the frequency of vibration. A is the amplitude of the shear waves.

The motion at the free surface would thus be $u_o = 2Ae^{i\Omega t}$ and the transfer function for the motion at depth z (for a specified motion at the free surface) would be

$$F = \frac{1}{2}(e^{ipz} + e^{-ipz})$$

Notice that if there is no internal damping in the soil, the function F will become cos $(\Omega z/c_s)$ with $c_s = \sqrt{G/\rho}$, the shear wave velocity of the soil. For any specific depth z = E the transfer function will become 0 at $\Omega = [(2n+1)\pi c_s]/2E$ or $f = [(2n+1)c_s]/4E$, which are the natural shear frequencies of a stratum of depth E. This implies that these frequencies would be entirely filtered out from the seismic motion and since the transfer function has a modulus less or equal to 1 over the complete frequency range, the amplitudes of motion would always be deamplified with depth. These statements are no longer true when there is some amount of internal damping in the soil, but for moderate values of damping the transfer function would still show some important oscillations with frequency.

It is also possible in the free field to define a pseudo-rotation (fig. 4)

$$\phi_B = \frac{u_A - u_B}{E}$$

For the case of the homogeneous stratum and no internal damping, this pseudo-rotation becomes

$$\phi_B = \frac{u_A}{E}\left(1 - \cos\frac{\Omega E}{c_s}\right) = 2\,\frac{u_A}{E}\sin^2\frac{\Omega E}{2c_s}$$

When considering a three-dimensional, cylindrical, rigid foundation embedded into the soil stratum, the vertically propagating shear waves will produce not only a horizontal translation of the base, but also a rotation. This rotation is caused by shear forces developed along the sidewalls-soil interface, due to the fact that the rigid sidewalls cannot deform in the same way as the surrounding soil would in the free field. The horizontal translation and the rotation were computed with the finite element formulation described earlier and divided by the amplitude of the horizontal motion at the free surface of the soil in the far field (one-dimensional solution). Seven different embedment ratios were studied, covering a range of values commonly encountered in the design of nuclear power plants. The corresponding values of the parameters were as indicated in Table 1.

Table 1

Case	E/R	H/R	E/H
1	0.5	1.5	1/3
2	0.5	2.0	1/4
3	0.5	2.5	1/5
4	1.0	1.5	2/3
5	1.0	2.0	1/2
6	1.0	2.5	2/5
7	1.5	2.0	3/4

5% internal damping, of a hysteretic nature, was assumed for all the cases.

Figures 5 through 11 show the amplitude of the transfer functions for the translational motion of the base of the foundation (3D solution). For the purposes of comparison, the corresponding results from the one-dimensional solution (motion at the level of the foundation in the far field) are also shown. The 3D solution follows very closely the 1D motion up to roughly 0.75 of the first natural frequency of the embedment region ($f_1 = c_s/4E$). After that point the 3D solution oscillates with only moderate amplitudes, while the 1D motion exhibits significant oscillations. Because of this the 1D solution would severely underestimate the motion in the region of the natural frequencies of the embedment region (f_n), while over-estimating it in the intervals between these frequencies ($f = 1/2(f_n+f_{n+1})$).

On the other hand, defining the input motion at the foundation level in the far field, as was suggested at one time, would result in a motion at the base of the foundation where the opposite would occur: the motion would be substantially amplified in the range of the natural frequencies f_n and deamplified in the intermediate ranges $(\frac{1}{2} f_n + \frac{1}{2} f_{n+1})$.

From inspection of these results it appears that a reasonable approximation to the 3D solution can be obtained by defining the transfer function for the horizontal translation as

$$F_u(\Omega) = \begin{cases} \cos \frac{\pi}{2} \frac{f}{f_1} & \text{for } f \leq 0.7\, f_1 \\ 0.453 & \text{for } f > 0.7\, f_1 \end{cases}$$

$$\text{with} \quad f_1 = \frac{c_s}{4E}.$$

Figures 12 through 18 show the amplitude of the transfer function for the rotation at the base of the foundation multiplied by the foundation radius R ($\phi R/u_A$). Shown in the same figures are the transfer functions for the one-dimensional pseudo rotation ϕ_B multiplied by the scaling factor 0.257E (this factor was obtained by comparing the average values of both functions). It can be seen that the agreement is very good in the low frequency range, but that it deteriorates again for larger frequencies where the one-dimensional solution exhibits much larger oscillations than the true rotation.

From inspection of these figures it appears that a reasonable approximation to the 3D solution can be obtained by defining the transfer function for the rotation as

$$F_\phi(\Omega) = \begin{cases} \frac{0.257}{R} (1 - \cos \frac{\pi}{2} \frac{f}{f_1}) & \text{for } f \leq f_1 \\ \frac{0.257}{R} & \text{for } f \geq f_1 \end{cases}$$

with f_1 as previously defined.

In these expressions ϕ is considered as positive clockwise.

In order to investigate the degree of approximation provided by these rules for a more realistic soil profile where the modulus increased with depth, one additional case was studied, with E/R = 1 and H/R = 2. The shear wave velocity varied from 0.5 c_s at the free surface to c_s at the foundation level and 1.1 c_s at the bottom of the soil profile. Figure 19 shows again the 3D and 1D transfer functions for the horizontal translation and the rotation as well as the suggested approximation. The results are still reasonable if f_1 is taken as the actual natural frequency of the embedment region.

Finally, in order to determine the effect of the foundation flexibility, the case E/R = 1, H/R = 2 was again considered, assuming a rigid base but modelling the sidewalls with finite elements with the elastic properties of concrete. Fig. 20 shows the results for this case and for the rigid foundation. It can be seen that the effect on the horizontal translation is negligible.

The base rotation on the other hand is reduced by 20 to 25%, a result which is intuitively logical. In the limiting case, if there were no sidewalls the foundation would still have a rotation but of opposite sign: this rotation would result from the fact that the lateral sides of the excavation would not have any shear stresses, while these stresses should exist in the far field solution. The actual conditions of the backfill would also have a significant influence on the magnitude of the rotation as well as the fact that some slippage should take place between the sidewalls and the soil during the vibration. Thus while the approximate expressions suggested above would yield results consistent with those provided by a direct solution of the combined soil-structure system (as provided by some of the computer programs used at present), in reality the rotation may be expected to be somewhat smaller.

It should be noticed that the rotation is an integral and important part of the base motion for the massless foundation. Ignoring it, while deamplifying the translational component, may lead to important errors on the unconservative side. To illustrate this point, figure 21 shows the results of a soil-structure interaction analysis performed on a structure with characteristics similar to those of typical containment buildings in nuclear power plants using the three-step approach and considering both components of motion (translation and rotation) and only the translation. Results obtained with a direct solution of the complete soil structure system were almost identical to those of the three-step approach with the two components of motion. The characteristics of the motions at the base of the structure (including the soil structure interaction effects)and at the top of the building are depicted in terms of their response spectra. It can be seen from the figure that the results of both analyses are very similar at the base of the structure, where the rotation has very little effect (the small differences are due to the coupling terms $K_{x\phi}$ in the foundation stiffness). At the top of the structure, however, the results ignoring the rotation are only about 50% of the "true" ones.

Figure 22 shows the corresponding results using the estimates of the translation and the rotation provided by the approximate rules suggested above. The agreement with the "true" solution is remarkably good, particularly at the top of the structure. Small differences exist in the response spectra at the base of the structure, but these differences are not significant, particularly if one takes into account the uncertainties involved in the definition of the design earthquake.

In all these analyses the dynamic stiffness matrix of the foundation, as a function of frequency, was the one computed from an appropriate finite element analysis, and the solution of the equations of motion for the structure on elastic foundation was carried out in the frequency domain.

DYNAMIC STIFFNESS OF EMBEDDED FOUNDATIONS

Approximate equations for the motion of a rigid cylindrical body completely embedded in an elastic spectrum were presented by Tajimi (18) in 1969. Novak and Beredugo (14) derived approximate analytical solutions for the vertical, horizontal and rocking stiffnesses of a rigid circular footing embedded in an elastic half space; frequency independent stiffness and damping parameters were approximated by Novak (13) and by Novak and Sachs (15). These solutions were used by Bielak (2) to study the behavior of structures with embedded foundations.

Finite element (or finite difference) solutions for strip footings and circular foundations embedded in a half space or a layer of finite depth were obtained at different times by Kaldjian (8), Krizek, Gupta and Parmelee (10), Waas (21), Urlich and Kuhlemeyer (19), Chang-Liang (3), Kausel (9), and Johnson, Christiano and Epstein (7).

Experimental studies on the dynamic behavior of embedded circular footings have been conducted and reported by Anandakrishnan and Krishnaswamy (1), Stokoe (17) and Erden (5).

The results used in this work were obtained with the same formulation and computer program developed by Kausel (9). As in the previous section (determination of the foundation motions), most of the studies were conducted for a uniform soil deposit of finite depth (resting on much stiffer rock-like material) and assuming a rigid foundation perfectly welded to the soil. The effects of variation of soil properties with depth and of the flexibility of the sidewalls were again investigated in a limited number of cases.

For the case of a steady state harmonic motion with frequency Ω the force displacement relationships can be written (for a rigid foundation) as

$$H = K_{xx}\ u + K_{x\phi}\ \phi$$

$$M = K_{\phi x}\ u + K_{\phi\phi}\ \phi$$

where H is the horizontal force, M the rocking moment, and u and ϕ the corresponding horizontal displacement and rotation. $K_{\phi x} = K_{x\phi}$.

Each stiffness term can be expressed in the form

$$K_{ij} = K^{o}_{ij}\ (k_{ij} + i a_o\ c_{ij})$$

where K°_{ij} is the static value

k_{ij} and c_{ij} are frequency depemdemt stiffness coefficients

$a_o = R/c_s$ is a dimensionless frequency

R is the radius of the circular foundation

c_s is the shear wave velocity of the soil.

If the soil has an internal damping ratio D, caused by hysteretic losses due to nonlinear behavior, the previous expression can be written approximately as

$$K_{ij} = K^{\circ}_{ij}\ (1 + 2iD)(k_{ij} + i\ a_o\ c_{ij})$$

The stiffness coefficients k_{ij}, c_{ij} are in rigor a function of the damping ratio D, but for typical values of this parameter and a hysteretic type damping (frequency independent) the dependence on D is small in the case of a half space and only significant around the fundamental frequency of the layer for a soil stratum of finite depth.

Static Stiffnesses. The effect of embedment on the static stiffnesses K°_{ij} was investigated first by considering the nine cases shown in Table 2. H is again the total depth of the stratum, R the radius of the foundation, and E the depth of embedment.

Table 2

Case	H/R	E/R	E/H
1	2	0.5	0.25
2	2	1.0	0.50
3	2	1.5	0.75
4	3	0.5	0.167
5	3	1.0	0.333
6	3	1.5	0.50
7	4	0.5	0.125
8	4	1.0	0.25
9	4	1.5	0.375

It is important to notice that when using finite elements the results will be a function of the mesh size. In order to obtain an accurate solution it is necessary thus to use a sufficiently fine mesh or, better even, to use two or three different meshes and to extrapolate the results. Following Kausel (9), three different meshes were used in this study with square elements whose size was equal to 1/4, 1/8, and 1/16 of the radius. Figure 23 shows the results obtained for a typical case (case 1 in table 2). It can be seen that since a linear displacement expansion was used for the finite elements, a linear extrapolation procedure seems to apply.

For a surface foundation Kausel (9) had suggested the approximate formulae

$$\overset{\circ}{K}_{xx} = \frac{8GR}{2-\nu}\left(1 + \frac{1}{2}\frac{R}{H}\right)$$

$$\overset{\circ}{K}_{\phi\phi} = \frac{8GR^3}{3(1-\nu)}\left(1 + \frac{1}{6}\frac{R}{H}\right)$$

$$\overset{\circ}{K}_{x\phi} = -0.03\ R\ \overset{\circ}{K}_{xx}$$

The extrapolated values resulting from this study for K_{xx} and $K_{\phi\phi}$ were divided by the above expressions and plotted versus R/H for different values of E/R, as shown in figures 24 and 25. It can be seen that for values of $R/H \leq 1/2$ and $E/R \leq 1$, the points fall almost exactly along straight lines. As the depth of the stratum decreases or the embedment increases beyond these values, the increase in the stiffnesses $\overset{\circ}{K}_{xx}$ and $\overset{\circ}{K}_{\phi\phi}$ is faster than linear as indicated schematically in figure 26. Most cases of practical interest would fall, however, within the range where the linear approximation is valid. Writing then the expressions for K_{xx} and $K_{\phi\phi}$ in the form

$$\overset{\circ}{K}_{xx} = \frac{8GR}{2-\nu}\left(1 + \frac{1}{2}\frac{R}{H}\right)\left(1 + \frac{\alpha}{\gamma}\frac{R}{H}\right)\gamma$$

$$\overset{\circ}{K}_{\phi\phi} = \frac{8GR^3}{3(1-\nu)}\left(1 + \frac{1}{6}\frac{R}{H}\right)\left(1 + \frac{\delta}{\beta}\frac{R}{H}\right)$$

the coefficients α/γ, γ, δ/β and β were computed and plotted versus E/R as shown in figure 27. From this figure the approximate expressions result:

$$\frac{\alpha}{\gamma} \simeq \frac{5}{4}\frac{E}{R} \qquad\qquad \gamma \simeq 1 + \frac{2}{3}\frac{E}{R}$$

$$\frac{\delta}{\beta} \simeq 0.7\,\frac{E}{R} \qquad\qquad \beta \simeq 1 + 2\,\frac{E}{R}$$

leading to the final formulae

$$\overset{\circ}{K}_{xx} = \frac{8GR}{2-\nu}\left(1 + \frac{1}{2}\frac{R}{H}\right)\left(1 + \frac{2}{3}\frac{E}{R}\right)\left(1 + \frac{5}{4}\frac{E}{H}\right)$$

$$\overset{\circ}{K}_{\phi\phi} = \frac{8GR^3}{3(1-\nu)}\left(1 + \frac{1}{6}\frac{R}{H}\right)\left(1 + 2\,\frac{E}{R}\right)\left(1 + 0.7\,\frac{E}{H}\right)$$

The term $\overset{\circ}{K}_{x\phi}/\overset{\circ}{K}_{xx}$ can be interpreted as an equivalent height of the center of stiffness of the foundation h. Since the rotation is assumed to be positive clockwise, a positive value of h would indicate that the center of stiffness is above the base of the foundation. It was found from the study that the term $h/R = \overset{\circ}{K}_{x\phi}/R\overset{\circ}{K}_{xx}$ varied almost linearly with E/R within the range of parameters studied and had a small dependence on H/R and on Poisson's ratio ν. (h/R decreases slightly with increasing H/R and increases with ν). This variation is illustrated in figure 28. For practical purposes, considering the uncertainty in the actual value of for any specific soil, an average expression can be used

$$\overset{\circ}{K}_{x\phi} = \overset{\circ}{K}_{\phi x} = \left(0.4\,\frac{E}{R} - 0.03\right) R\overset{\circ}{K}_{xx} \qquad \text{for } \frac{E}{H} \leq 0.5$$

In order to investigate the effect of the flexibility of the foundation and in particular that of the sidewalls, the case E/R = 1, ν = 1/3 was again studied for the three values of H/R. The base of the foundation was still considered rigid, but the sidewalls were modeled with finite elements with the properties of concrete. The results are shown in Table 3.

Table 3 - Effect of Flexible Sidewalls

		H/R = 2	H/R = 3	H/R = 4
$\frac{\overset{\circ}{K}_{xx}}{GR}$	RIGID SIDEWALL	16.84	13.75	12.60
	FLEX. SIDEWALL	15.72	12.91	11.89
$\frac{\overset{\circ}{K}_{\phi\phi}}{GR^3}$	RIGID SIDEWALL	18.30	16.12	15.51
	FLEX. SIDEWALL	14.66	12.88	12.43
$\frac{\overset{\circ}{K}_{x\phi}}{GR^2}$	RIGID SIDEWALL	5.79	4.64	4.16
	FLEX. SIDEWALL	3.91	3.12	2.79

As in the case of the foundation motion, the effect of the flexibility of the sidewalls is more important for the rotation than for the translation. The reduction in the horizontal stiffness is only of the order of 7%, while the rotational stiffness decreases by about 20% and the coupling term $\overset{\circ}{K}_{x\phi}$ by nearly 30%. The actual conditions of the soil in the backfill and the possible separation between the sidewalls and the soil during the vibration would again contribute to a reduction in the effective embedment, but an assessment of this reduction is difficult and would require additional studies with a nonlinear soil model.

The case H/R = 2, E/R = 1, $\nu = 1/3$ was studied again considering a soil profile with variable properties. As in the previous section, it was assumed that the shear wave velocity of the soil increased from a value of 0.5 c_s at the surface to c_s at the foundation level and $1/c_s$ at the bottom. Expressing the stiffness in terms of the shear modulus corresponding to c_s, table 4 compares the results obtained for the uniform and the variable profiles.

Table 4

	Uniform soil profile	Variable soil profile
$\frac{\overset{\circ}{K}_{xx}}{GR}$	16.84	15.52
$\frac{\overset{\circ}{K}_{\phi\phi}}{GR^3}$	18.30	15.46
$\frac{\overset{\circ}{K}_{x\phi}}{GR^2}$	5.79	3.97

It can be seen that the increase in the stiffness of the soil below the foundation is less significant for the case considered than the reduction in the modulus over the embedment. Again the effect is more marked for the terms $K_{x\phi}$ and $K_{\phi\phi}$ than for K_{xx} (the results are in fact very similar to those obtained for the flexible sidewalls).

Figure 29 shows a comparison of the static stiffnesses (divided by those of a surface foundation) predicted from the approximate expressions suggested above and those that would result from the work of Urlich and Kuhlemeyer (19). The solution of Urlich and Kuhlemeyer was intended to apply to the case of a half space, but it is based on a finite element model with viscous dashpots at the boundaries. Since these dashpots are not operative for the static case, the values of the static stiffnesses derived from the study correspond in fact to a stratum of finite depth (H/R = 6) and a domain which is also finite in the lateral direction (it should be noticed that their results do not converge to the correct analytical solution as the embedment tends to zero). Considering these facts, the agreement between the two solutions is very good, particularly for the terms $K_{\phi\phi}$ and h/R (or $K_{x\phi}/RK_{xx}$). The results for K_{xx} show small discrepancies, particularly in their trend: although the differences are not significant for practical purposes, it would appear that the results from Urlich and Kuhlemeyer's work correspond to a shallower stratum for lower values of the embedment ratio and approach the half space solution as E/R increases.

Figure 30 compares the values predicted by the approximate formulae with those obtained by Johnson, Christiano and Epstein (7) using a finite element model with triangular elements and lateral boundaries on roller supports. It should be noticed again that their solution does not converge to the analytical values for a surface foundation on a half space. The agreement in the trend of the results is very good, but the stiffnesses resulting from Johnson, Christiano and Epstein's work are sightly larger: this may be due to the use of triangular finite elements without an appropriate extrapolation to correct for mesh size (the model would be naturally too stiff).

It is believed that the formulae suggested here will provide an excellent approximation within the range of parameters for which they apply ($H/R \geq 2$, $E/R \leq 1$, $E/H \leq 1/2$). In practice, however, it may be expected that the values of $K_{\phi\phi}$ and $K_{x\phi}$ particularly should be somewhat smaller than those given by the formulae because of the other effects discussed above. A reduction in these values should be, however, accompanied by a similar reduction in the foundation rotation (due to the seismic motions).

Dynamic Stiffness Coefficients

The dynamic stiffness coefficients k_{ij} c_{ij} were obtained for the same cases presented above by computing the stiffnesses K_{ij} as a function of the dimensionless frequency a_0 and dividing them by the factor $\overset{o}{K}_{ij}(1+2iD)$. A value of $D = 0.05$ was considered. Figure 31 shows typical results for one of the cases ($H/R = 3$, $E/R = 1$). Shown in the figure are the swaying and rocking coefficients for the embedded foundation, the same foundation on the surface of a soil stratum with the total depth H and a surface foundation on a half space. The last results are obtained from the analytical solution presented by Veletsos and Wei (20), but the imaginary terms below the fundamental frequency of the stratum are modified according to the rules suggested later.

It can be seen from this figure that for the case of a finite stratum the term k_{xx} shows oscillations with frequency corresponding to the existence of natural frequencies for the soil deposit (if the soil had no internal damping, the stiffness should become zero at a value $a_o = (2\pi/4)(R/H) = \pi/6$ for the case shown). These oscillations decrease, however, as the internal damping in the soil increases. As a first approximation, if some amount of hysteretic damping is expected, due to the seismic excitation itself or to the foundation motion, one can take the half space solution without a significant loss of accuracy (although it should be noticed that as the frequency a_o increases, the effect of the layer depth in increasing the stiffness through the term $1 + 1/2\ (R/H)$ tends to disappear). One can assume therefore $k_{xx} \simeq 1$.

The agreement between the rocking stiffness coefficients $k_{\phi\phi}$ for the three cases is better than for the term k_{xx} and use of the half space solution seems quite appropriate. As an approximation for values of Poisson's ratio between 0 and 0.4 one can take

$$k_{\phi\phi} = 1 - 0.2\ a_o \qquad \text{for } a_o \leq 2.5$$

$$\text{and} \qquad k_{\phi\phi} \simeq 0.5 \qquad \text{for } a_o \geq 2.5.$$

For values of ν of the order of 0.45 to 0.5, $k_{\phi\phi} \simeq 1 - 0.2\ a_o$ over the complete range of interest.

The complex stiffness coefficients c_{xx} $c_{\phi\phi}$ are associated with the radiation damping (loss of energy by radiation of waves away from the foundation). For the case of a half space, the solutions presented by Veletsos and Wei (20) can be approximated by

$$c_{xx} \simeq 0.60$$

$$c_{\phi\phi} \simeq \frac{0.35\ a_o^2}{1 + a_o^2}$$

(More accurate analytical expressions for the coefficients k_{xx} $k_{\phi\phi}$ c_{xx} and $c_{\phi\phi}$ have been obtained by Veletsos and Verbic (21) in terms of Poisson's ratio ν, and can be used in practice without any increase in complexity if the value of ν is known).

For a surface foundation on a soil stratum of finite depth (resting on rigid rock), the above expressions for c_{xx} and $c_{\phi\phi}$ can again be used as an approximation above the fundamental frequencies of the stratum ($a_{o1} = \pi R/2H$ or $f_{o1} = R/4H$ for c_{xx} and $a_{o2} = a_{o1}\ (c_p/c_s)$ for $c_{\phi\phi}$ where c_p is the P wave velocity of the soil and c_s the shear wave velocity. Below this frequency there is no lateral radiation of waves (the vertical radiation is prevented by the rigid bottom), and if the soil were perfectly elastic c_{xx} and $c_{\phi\phi}$ should be zero. If the soil has some internal damping D, of a hysteretic nature, associated with nonlinear behavior, a transition curve should be used from $a_o = 0$ to $a_o = a_{o1}$ or a_{o2} respectively. Figure 32 shows the transition curves for the same case of Figure 31 (with D = 0.05). The dotted line corresponds to the approximation

$$c_{xx} \simeq 0.65\ D \frac{\alpha}{1-(1-2D)\alpha^2} \qquad \text{for } \alpha = \frac{a_o}{a_{o1}} \leq 1$$

$$c_{\phi\phi} \simeq 0.50D \frac{\alpha}{1-(1-2D)\alpha^2} \text{ but } \leq \frac{0.35a_o^2}{1+a_o^2} \qquad \text{for } \alpha = \frac{a_o}{a_{o1}} \leq \frac{c_p}{c_s}$$

The results provided by these expressions will be in general slightly on the conservative side, particularly in the neighborhood of the transition point ($a_o = a_{o1}$ or a_{o2} where there is a jump in the proposed solution).

For an embedded foundation in a finite stratum, it can be seen from figure 31 that the same type of transition must take place. The values of c_{xx} above $a_o = a_{o1}$ are, however, somewhat larger than those of a surface foundation and so are the values of $c_{\phi\phi}$ over most of the frequency range. Embedment will thus increase not only the static stiffnesses, but also the amount of radiation damping. This increase is sensitive, however, to the conditions of the backfill, the flexibility of the sidewalls and the bonding (or debonding) between the foundation and the surrounding soil. Without further studies on these effects, it is therefore recommended to use for the dynamic stiffness coefficients of an embedded foundation.

k_{xx}, $k_{\phi\phi}$ same as the half space solution for a surface foundation, using the expressions given above or the more accurate ones by Veletsos and Wei (20) or Veletsos and Verbic (21).

$$c_{xx} = \begin{cases} 0.65D \dfrac{\alpha}{1-(1-2D)\alpha^2} & \text{for } \alpha = \dfrac{a_o}{a_{o1}} \leq 1 \\ \text{half space solution for a surface foundation for } a_o > a_{o1} = \dfrac{\pi R}{2H} \end{cases}$$

$$c_{\phi\phi} = \begin{cases} 0.50D \dfrac{\alpha}{1-(1-2D)\alpha^2} \text{ but } \leq \dfrac{0.35a_o^2}{1+a_o^2} & \text{for } \alpha = \dfrac{a_o}{a_{o1}} \leq \dfrac{c_p}{c_s} \\ \text{half space solution for a surface foundation for } a_o > a_{o1} \dfrac{c_p}{c_s} \end{cases}$$

The stiffness coefficients for the coupling term $K_{x\phi}$ can be better evaluated by studying the term $h/R(K_{x\phi}/RK_{xx})$. For the cases studied it was found that this ratio is nearly a real number and almost independent of frequency. It is thus recommended to take the same expression as for the static values

$$K_{x\phi} = (0.4 \frac{E}{R} - 0.03)\ RK_{xx}$$

To illustrate the degree of approximation provided by these rules, the same structure considered in the previous section was analyzed using the three-step approach with the "exact" foundation motions but the approximate stiffnesses. The results in terms of response spectra of the foundation level and at the top of the structure are shown in figure 33. It can be seen that the spectra at the base are almost identical. At the top of the structure, on the other hand, the use of the approximate stiffnesses gives a peak response which is about 30% higher than the "correct" one. This is due to the fact that the natural frequency of the soil-structure system was of the order of 2.4 cps, slightly smaller than the dilatational frequency of the stratum (2.5 cps). The radiation damping in rocking given by the approximate expressions (applicable to a surface foundation) is therefore very small, while that resulting with the embedment effect would be more significant. The question remains, however, as to whether the full effect of embedment would actually take place in practice and thus as to whether the "correct" solution or the approximate one is more realistic. Additional studies made with deeper soil strata, in which the resonant shear beam and dilatational frequencies of the stratum were smaller than the fundamental rocking-swaying frequency of the soil-structure system, revealed a much better agreement between true and approximate solutions.

Figure 34 shows, finally, the results obtained using both the approximate foundation motions and the approximate foundation stiffnesses (for the same structure). The same comments made before when using only the approximate motions or the approximate stiffnesses apply here. On the other hand, analyses made using directly the half space stiffnesses and limiting the damping to 10% of critical (a procedure which has been suggested sometimes) and/or subjecting the system to the control motion directly at the base of the foundation gave results in gross disagreement with any of these solutions.

CONCLUSIONS AND RECOMMENDATIONS

It was the purpose of this work to derive simplified rules to account for the effect of foundation embedment in a soil-structure interaction analysis using the three-step or substructure approach. It is believed that the rules suggested will provide in general results in good agreement with those of a direct or one-step solution. It is important to notice that for a consistent solution the motions at the base of a massless foundation, computed in step 1, must include both a translation and a rotation. Neglecting the latter could result in important errors on the unconservative side. In addition, the translation, while exhibiting a deamplification from the motion at the free surface, has much less frequency sensitivity than would be implied by a one-dimensional solution. The foundation stiffnesses will increase due to embedment and so will, to some extent, the amount of radiation damping. It appears, however, that it is more important to reproduce correctly the static values of the stiffnesses than their complete frequency variations and one can, without serious error, assume the same functions of frequency (dynamic stiffness coefficients) as for a surface foundation on an elastic half space (if one expects some amount of internal soil damping). The only point of concern in this respect is the variation of the imaginary stiffness coefficients (and particularly the rocking one) below the fundamental frequencies of the stratum when assuming a rigid bottom (if there is in fact an abrupt transition in soil properties, with a much stiffer, rock-like material, underlying a soft soil layer). The formulae suggested here will give results generally on the conservative side, particularly in the neighborhood of the soil frequencies.

The rotation at the base of the massless foundation due to the seismic input and the stiffness functions $\overset{o}{K}_{x\phi}$ $\overset{o}{K}_{\phi\phi}$ and $c_{\phi\phi}$ are particularly sensitive to the flexibility of the sidewalls, the actual conditions of the backfill and the possible debonding between the sidewalls and the soil during the vibration. All these effects will tend to decrease their values (reducing the effective embedment).

More studies should be conducted to assess the importance of these effects (normally neglected in a direct solution) using a nonlinear soil model.

It would seem in addition that the studies reported in the section on foundation motions should be extended to the consideration of other types of waves instead of only shear waves propagating vertically. In this way rules might be derived to obtain average-type motions (including torsional components) at the foundation base.

REFERENCES

1. Anandakrishnan, M. and Krishnaswamy, N.R., "Response of Embedded Footings to Vertical Vibrations," Journal of the Soil Mech. and Found. Div. ASCE, Oct. 1973.

2. Bielak, J., "Dynamic Behavior of Structures with Embedded Foundations," Earthquake Engineering and Structural Dynamics, Vol. 3, No. 3, Jan.-March, 1975.

3. Chang Liang, V., "Dynamic Response of Structures in Layered Soils," Research Report R74-10, Civil Engineering Department, M.I.T., Jan. 1974.

4. Elsabee, F., "Static Stiffness Coefficients for Circular Foundations Embedded in an Elastic Medium," Thesis presented to the Civil Engineering Department of M.I.T. in partial fulfillment of the requirements for the M.S. degree, 1975.

5. Erden, S.M., "Influence of Shape and Embedment on Dynamic Foundation Response," Thesis submitted to the Graduate School of the University of Massachusetts at Amherst in partial fulfillment of the requirements for the Ph.D. degree 1974.

6. Gutierrez, J.A., "A Substructure Method for Earthquake Analysis of Structure-Soil Interaction," Report No. EERC 76-9, University of California, Berkeley, April 1976.

7. Johnson, G.R., Christiano, P. and Epstein, H.I., "Stiffness Coefficients for Embedded Footings," Proc. ASCE Power Div. Specialty Conf., Denver, Col., Aug. 1974.

8. Kaldjian, J.M., "Torsional Stiffness of Embedded Footings," Journal Soil Mech. and Found. Div., ASCE, July 1971.

9. Kausel, E., "Forced Vibrations of Circular Foundations on Layered Media," Report R74-11, Civil Engineering Department, M.I.T., Jan. 1974.

10. Krizek. R.J., Gupta, D.C., Parmelee, R.A., "Coupled Sliding and Rocking of Embedded Foundations," Journal of the Soil Mechanics and Foundations, Div., ASCE, 1972.

11. Lysmer, J., Seed, H.B., Udaka, T., Hwang, R.N. and Tsai, C.F., "Efficient Finite Element Analysis of Seismic Soil Structure Interaction," Report EERC 75-34, University of California, Berkeley, Nov. 1975.

12. Morray, J.P., "The Kinematic Interaction Problem of Embedded Circular Foundations," Thesis presented to the Civil Engineering Department of M.I.T. in partial fulfillment of the requirements for the M.S. degree, 1975.

13. Novak, M., "Vibrations of Embedded Footings and Structures," Preprint 2029, ASCE Nat. Struct. Engrg. Meeting, San Francisco, California, April 1973.

14. Novak, M. and Beredugo, Y.O., "The Effect of Embedment on Footing Vibrations," Proc. First Canadian Conf. on Earthquake Engrg. Research, Vancouver, May 1971.

15. Novak, M. and Sachs, K., "Torsional and Coupled Vibrations of Embedded Footings," Int. Journal of Earthquake Engineering and Structural Dynamics, Vol. 2, No. 1, July-Sept. 1973.

16. Roesset, J.M. and Whitman, R.V., "Theoretical Background for Amplification Studies," Report R69-15 , Civil Engineering Department, M.I.T., March 1969.

17. Stokoe, K.H. II, "Dynamic Response of Embedded Foundations," Thesis submitted in partial fulfillment of the requirements for the Ph.D. degree, University of Michigan, Jan. 1972.

18. Tajimi, H., "Dynamic Analysis of a Structure Embedded in an Elastic Stratum," Proc. 4th World Conf. on Earthquake Engineering, Santiago, Chile, 1969.

19. Urlich, C.M. and Kuhlemeyer, R.L., "Coupled Rocking and Lateral Vibrations of Embedded Footings," Can. Geotech. Journal, Vol. 10, No. 2, May 1973.

20. Veletsos, A.S. and Wei, Y.T., "Lateral and Rocking Vibration of Footings," Journal of the Soil Mech. and Found. Div. ASCE, Vol. 97, Sept. 1971.

21. Veletsos, A.S. and Verbic, B,"Impulse Response Functions for Elastic Foundations," Report No. 5, Department of Civil Engineering, Rice University, Sept. 1972.

22. Waas, G., "Linear Two-Dimensional Analysis of Soil Dynamics Problems in Semi-Infinite Layered Media," Thesis submitted in partial fulfillment of the requirements for the Ph.D. degree - University of California, Berkeley, 1972.

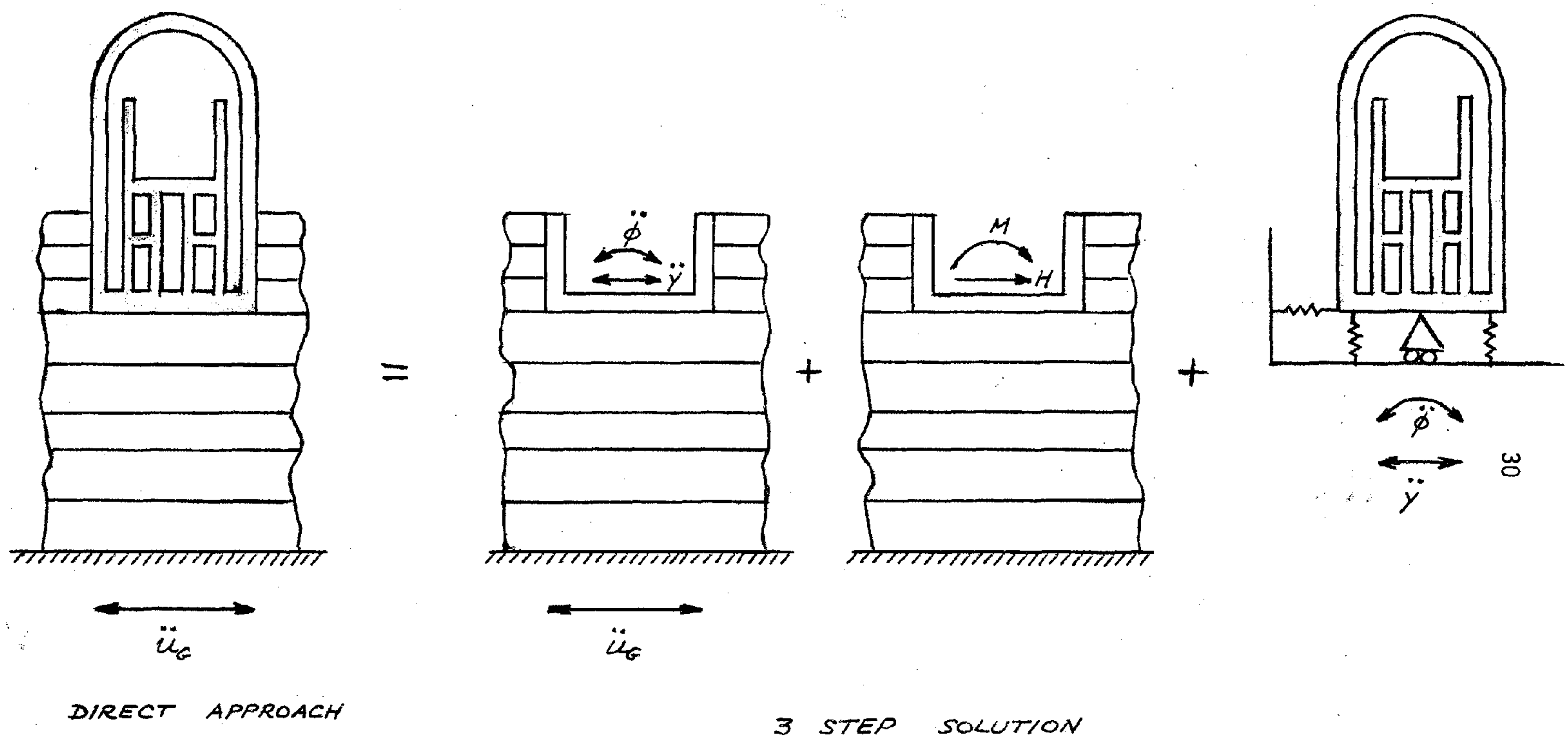

FIGURE 1 - METHODS OF SOLUTION

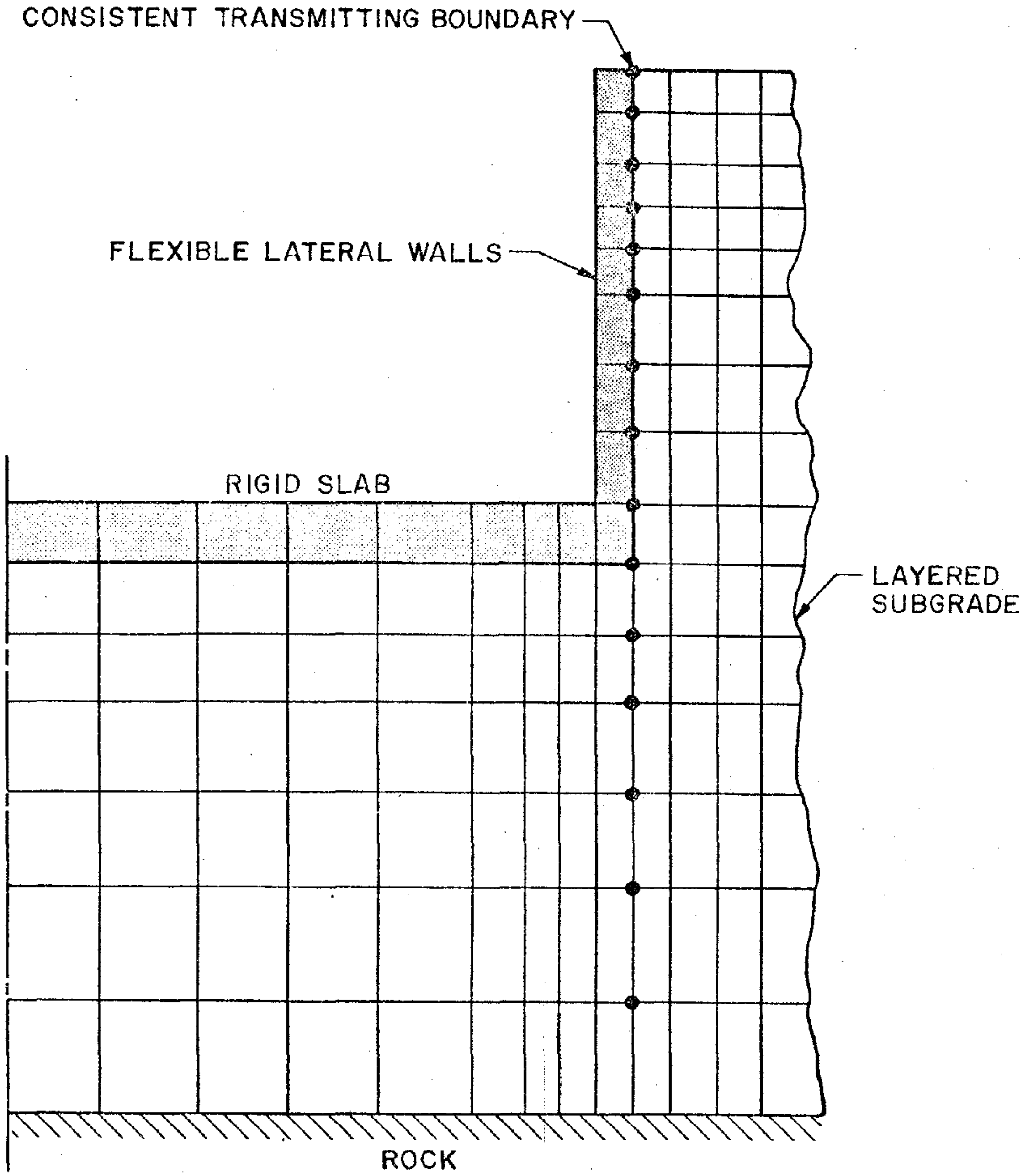

FIGURE 2

FINITE ELEMENT IDEALIZATION OF MASSLESS FOUNDATION

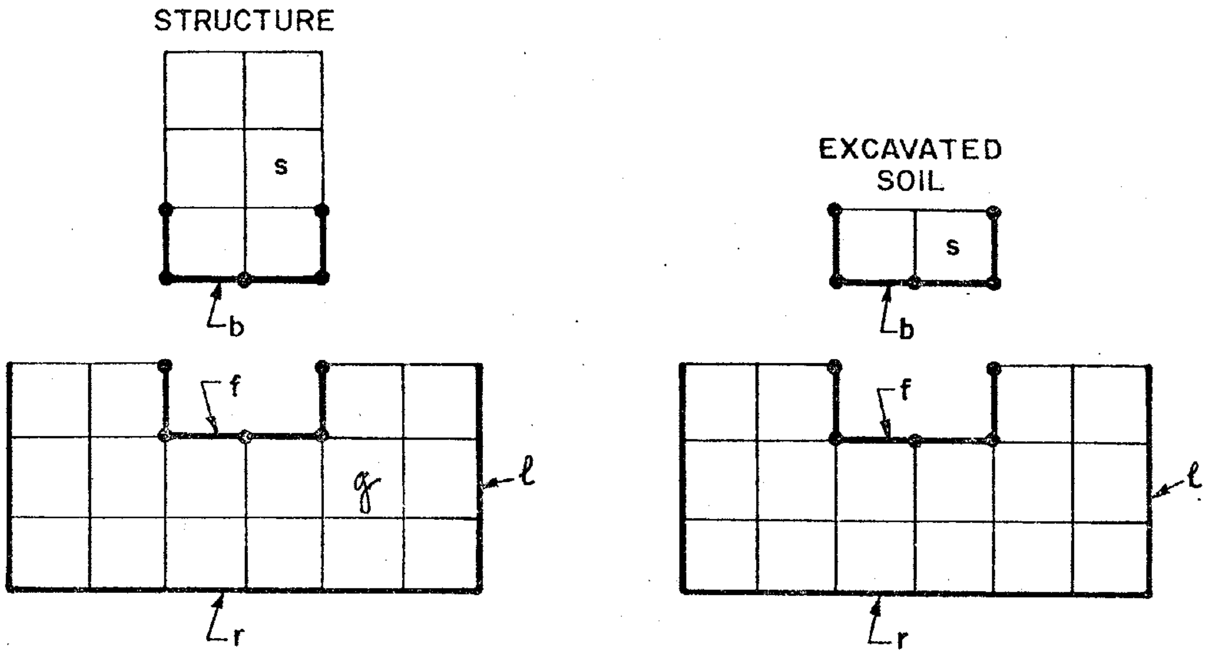

a) SOIL STRUCTURE INTERACTION PROBLEM

b) FREE FIELD PROBLEM

FIGURE 3

SUBSTRUCTURE THEOREM

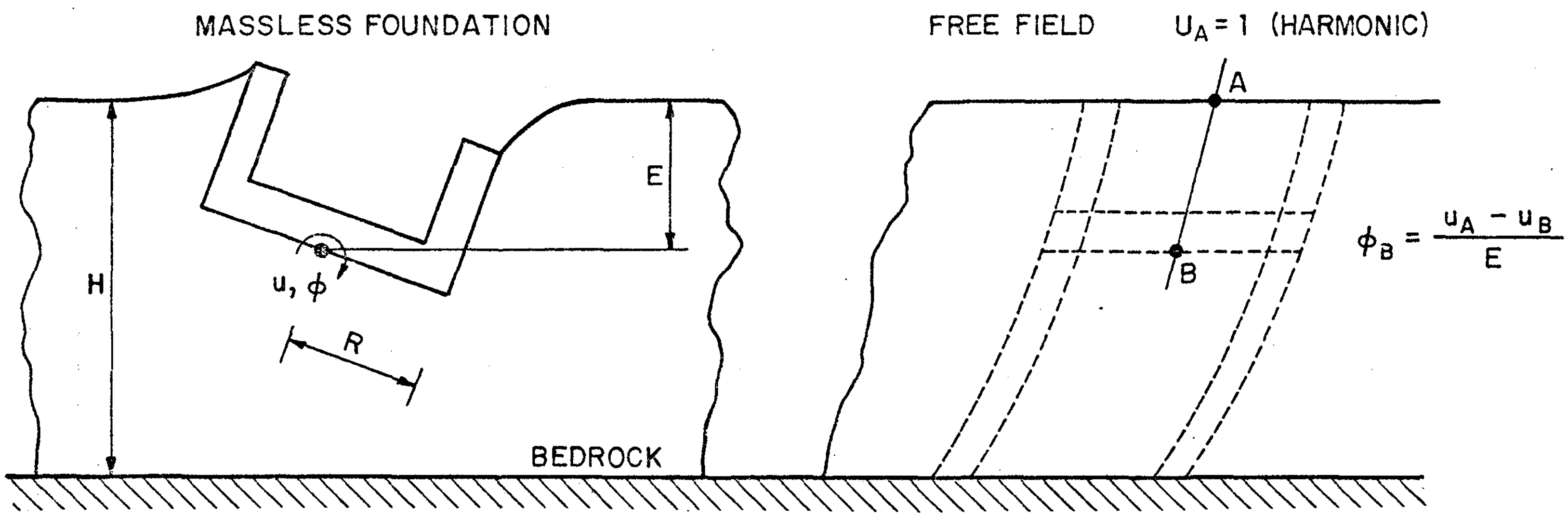

FIGURE 4
KINEMATIC INTERACTION PROBLEM

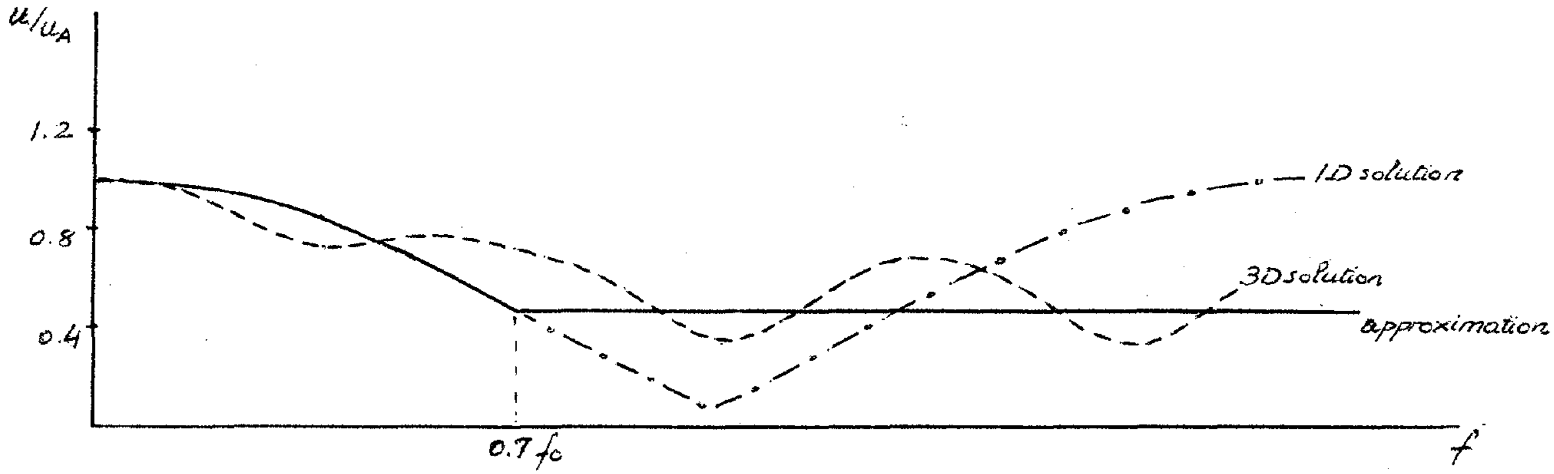

FIGURE 5. TRANSFER FUNCTIONS FOR HORIZONTAL MOTION. Case 1

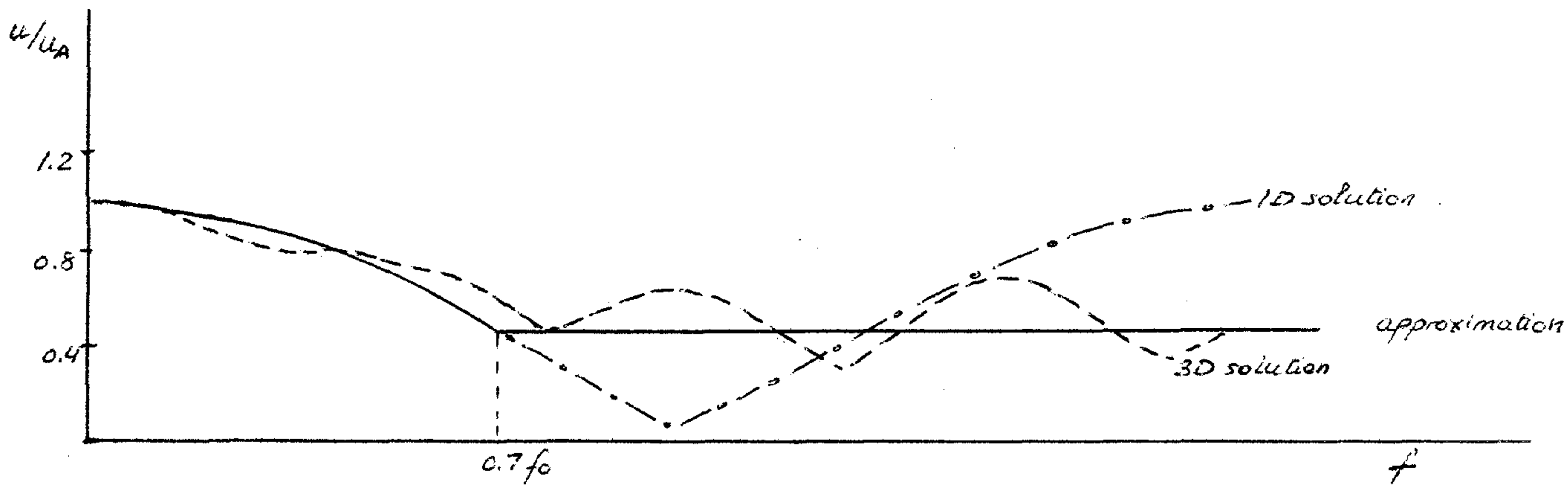

FIGURE 6. TRANSFER FUNCTIONS FOR HORIZONTAL MOTION Case 2

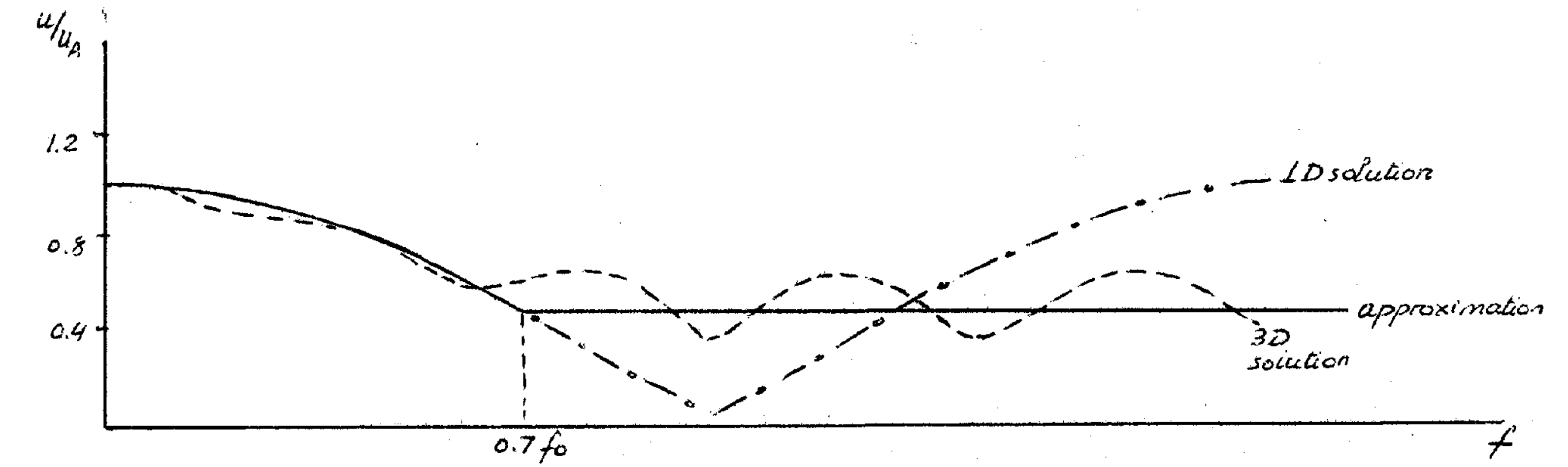

FIGURE 7 TRANSFER FUNCTIONS FOR HORIZONTAL MOTION - Case 3

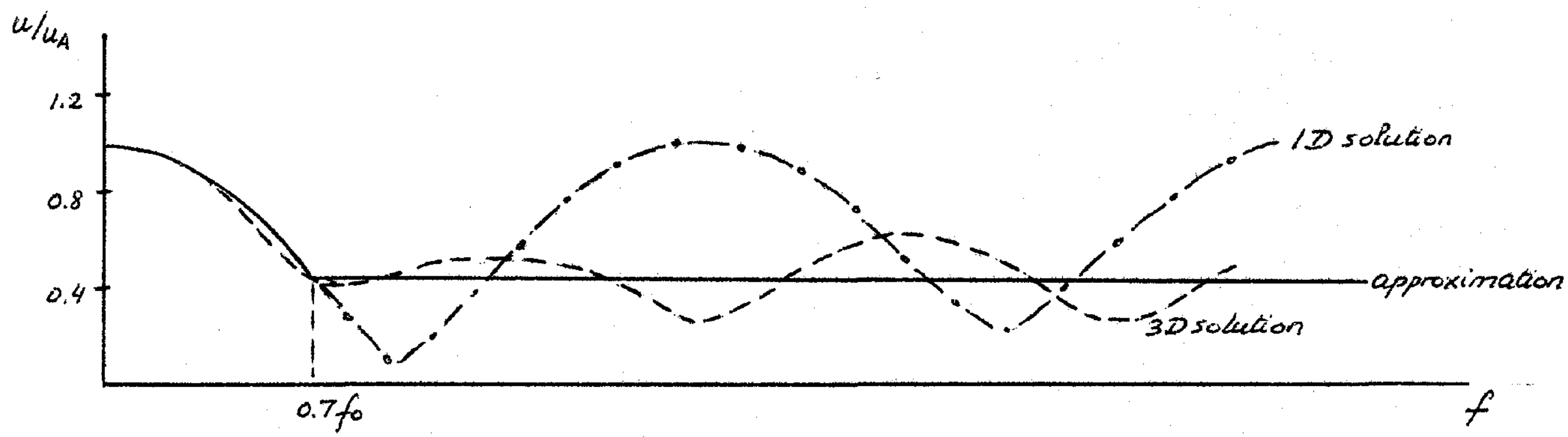

FIGURE 8 TRANSFER FUNCTIONS FOR HORIZONTAL MOTION - Case 4

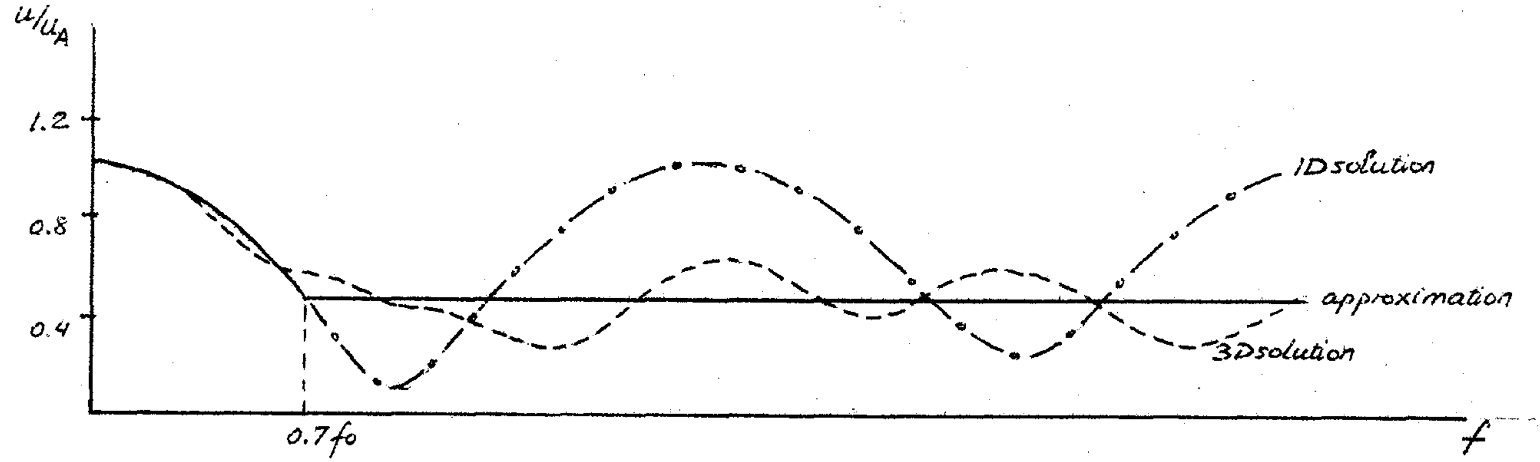

FIGURE 9. TRANSFER FUNCTIONS FOR HORIZONTAL MOTION - Case 5

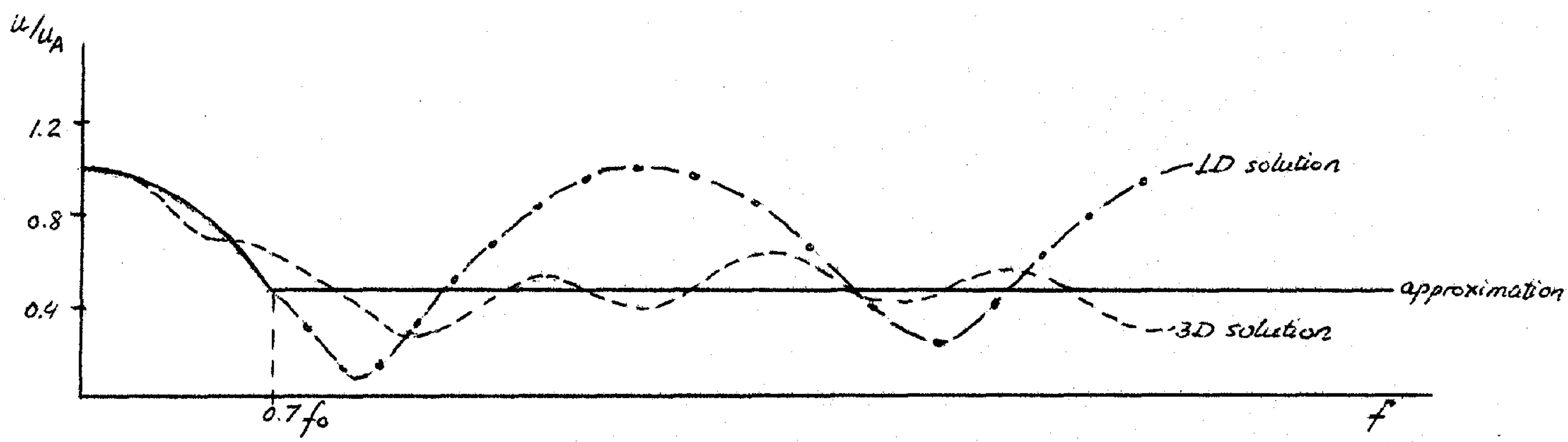

FIGURE 10 - TRANSFER FUNCTIONS FOR HORIZONTAL MOTION - Case 6

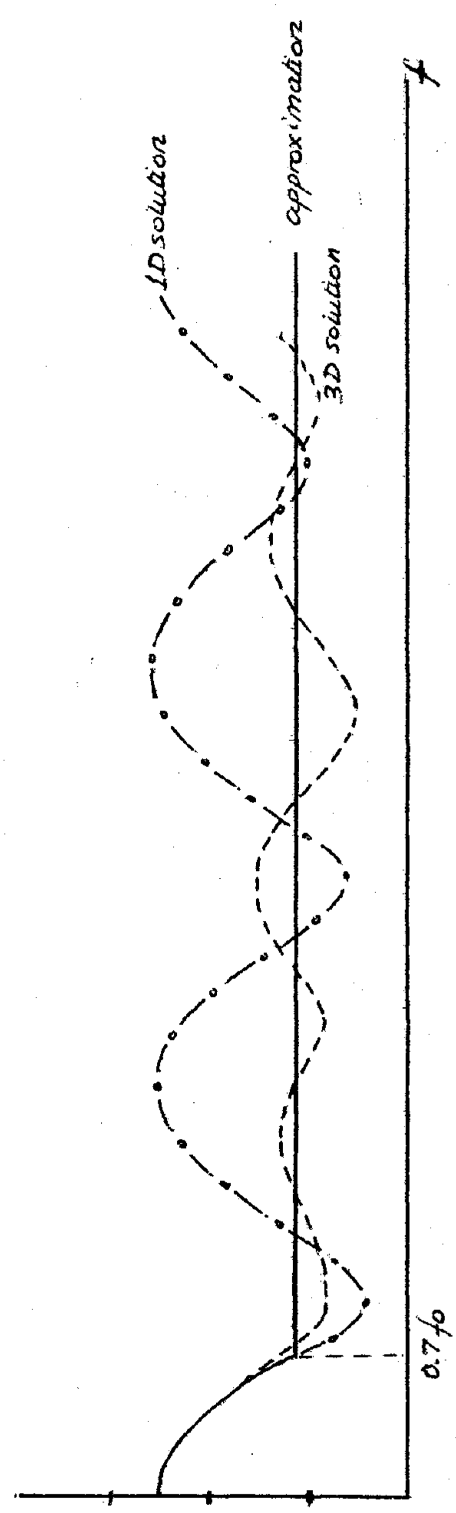

FIGURE 11 - TRANSFER FUNCTIONS FOR HORIZONTAL MOTION - Case 7

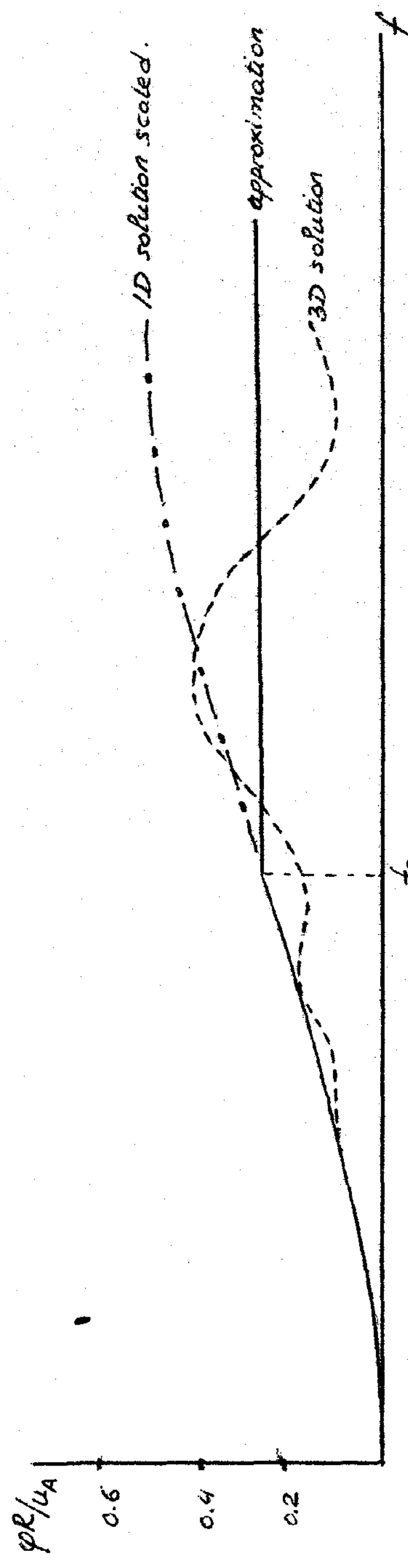

FIGURE 12 - TRANSFER FUNCTIONS FOR ROTATION - Case 1.

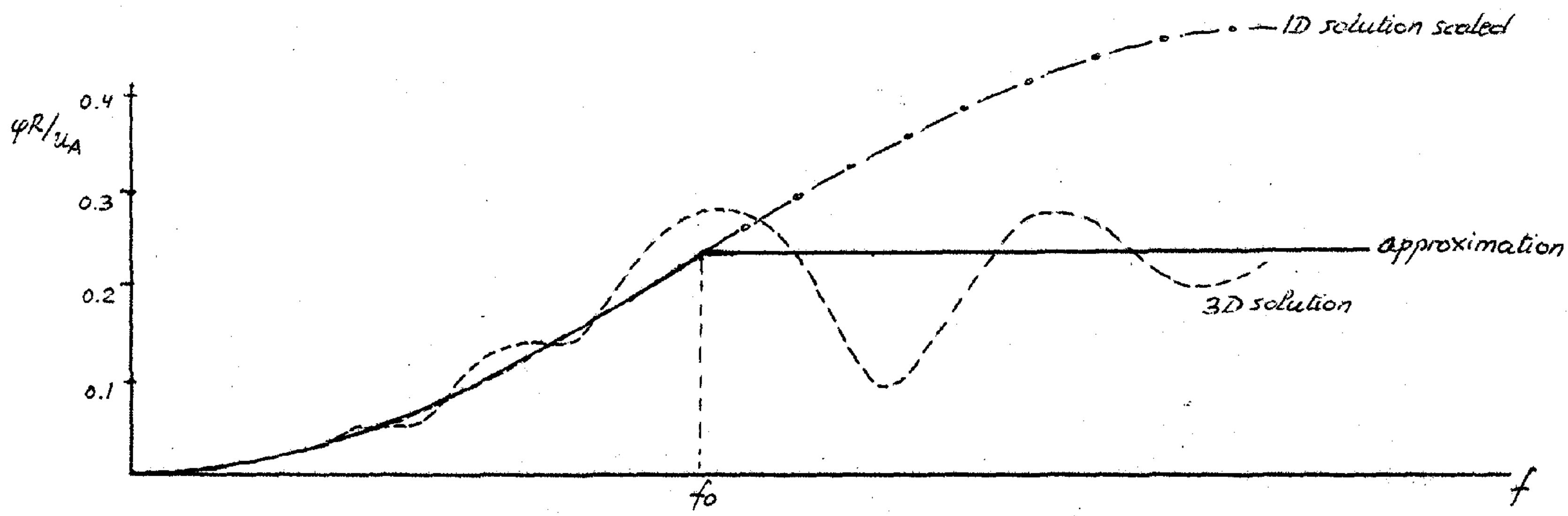

FIGURE 13 - TRANSFER FUNCTIONS FOR ROTATION - Case 2

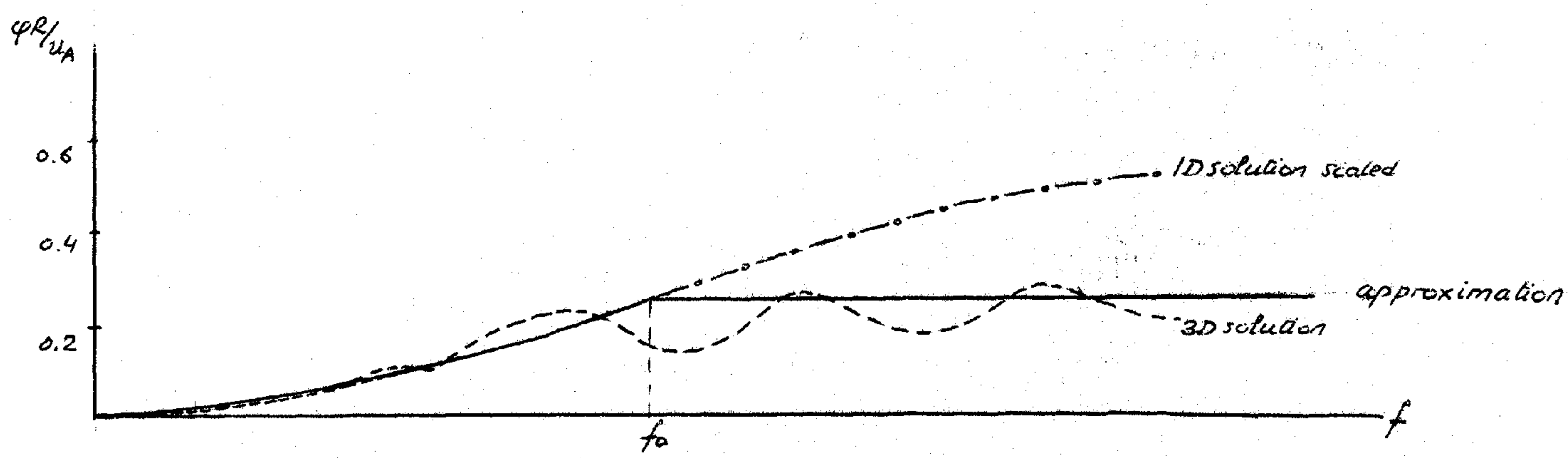

FIGURE 14 - TRANSFER FUNCTIONS FOR ROTATION - Case 3

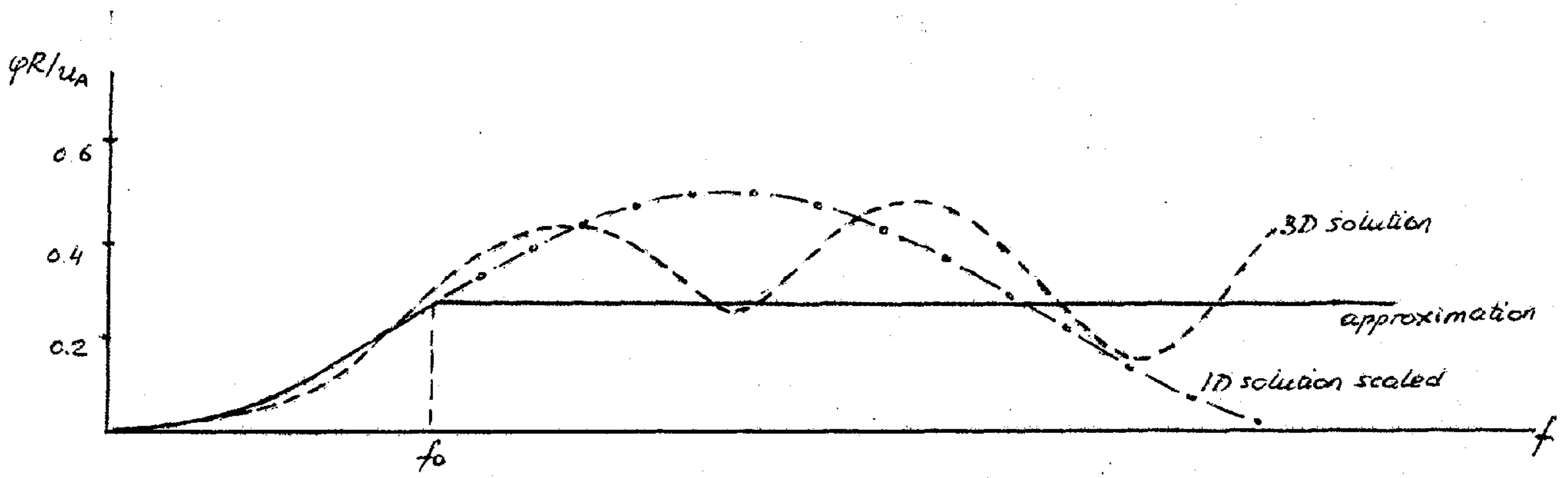

FIGURE 15 . TRANSFER FUNCTIONS FOR ROTATION. Case 4

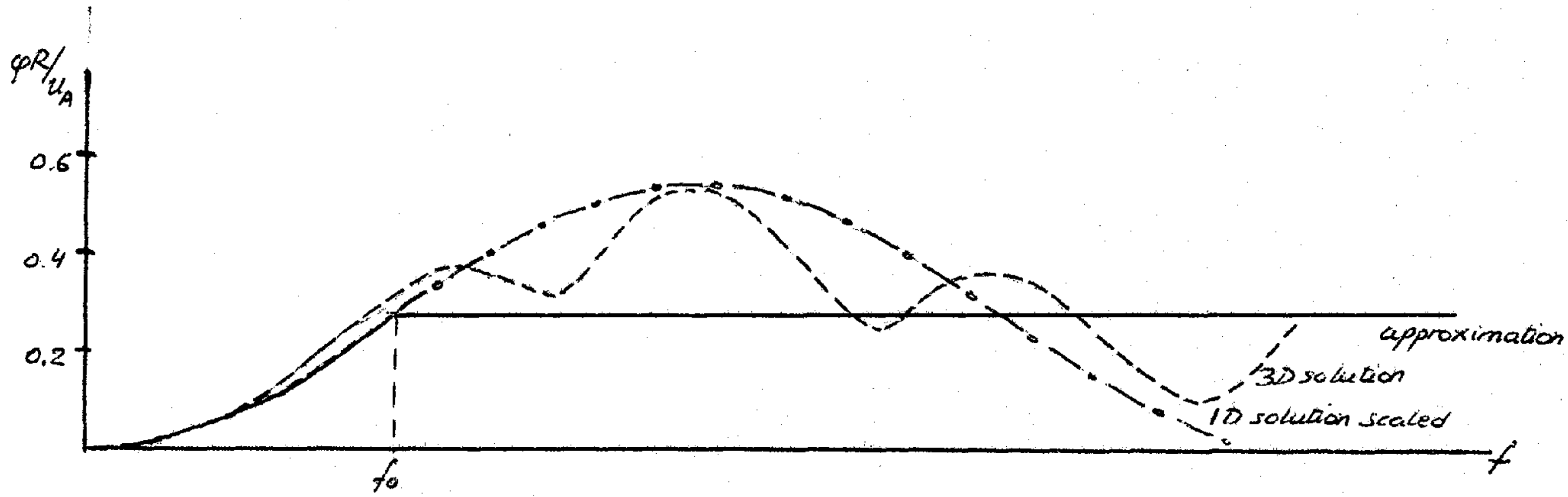

FIGURE 16 . TRANSFER FUNCTIONS FOR ROTATION. Case 5

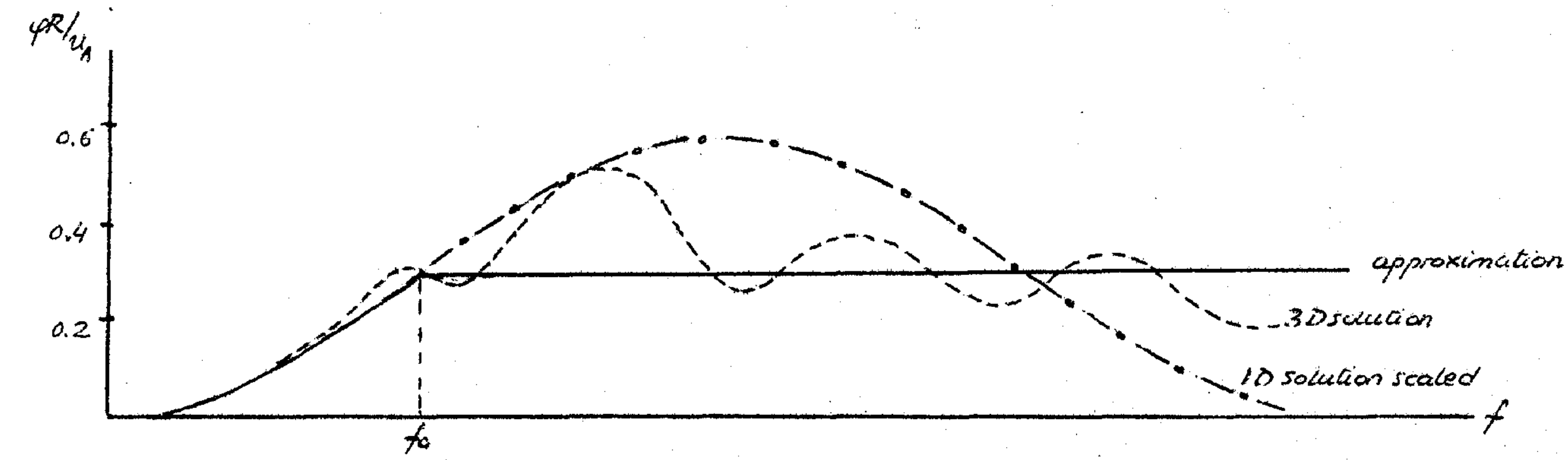

FIGURE 17. TRANSFER FUNCTIONS FOR ROTATION. Case 6

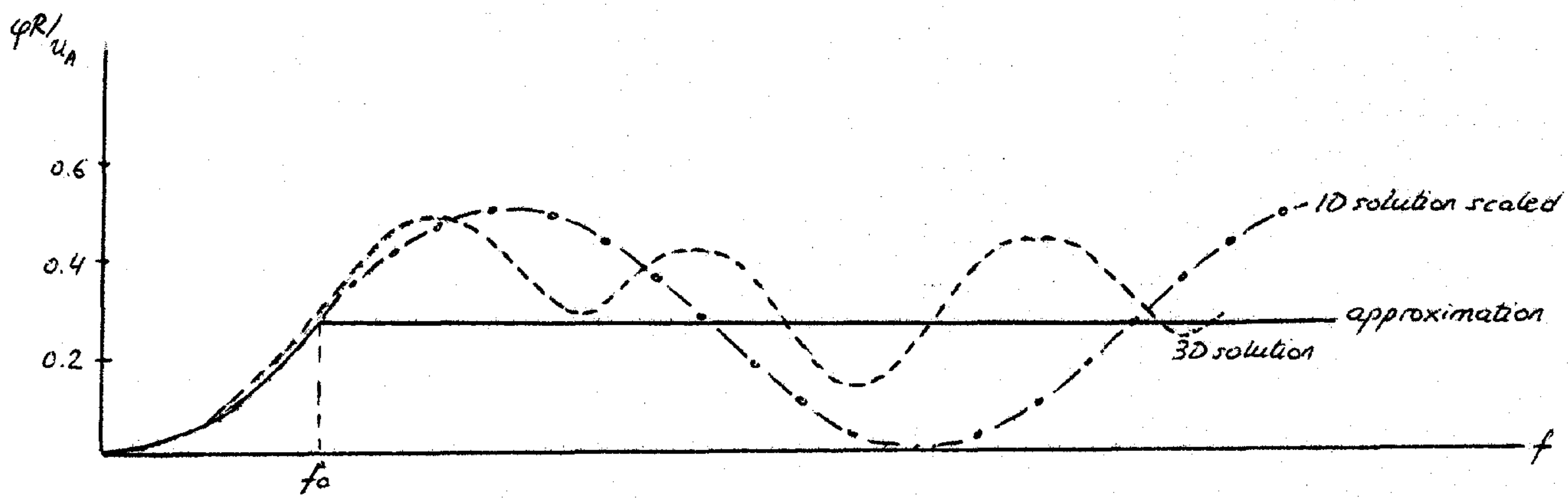

FIGURE 18. TRANSFER FUNCTIONS FOR ROTATION. Case 7

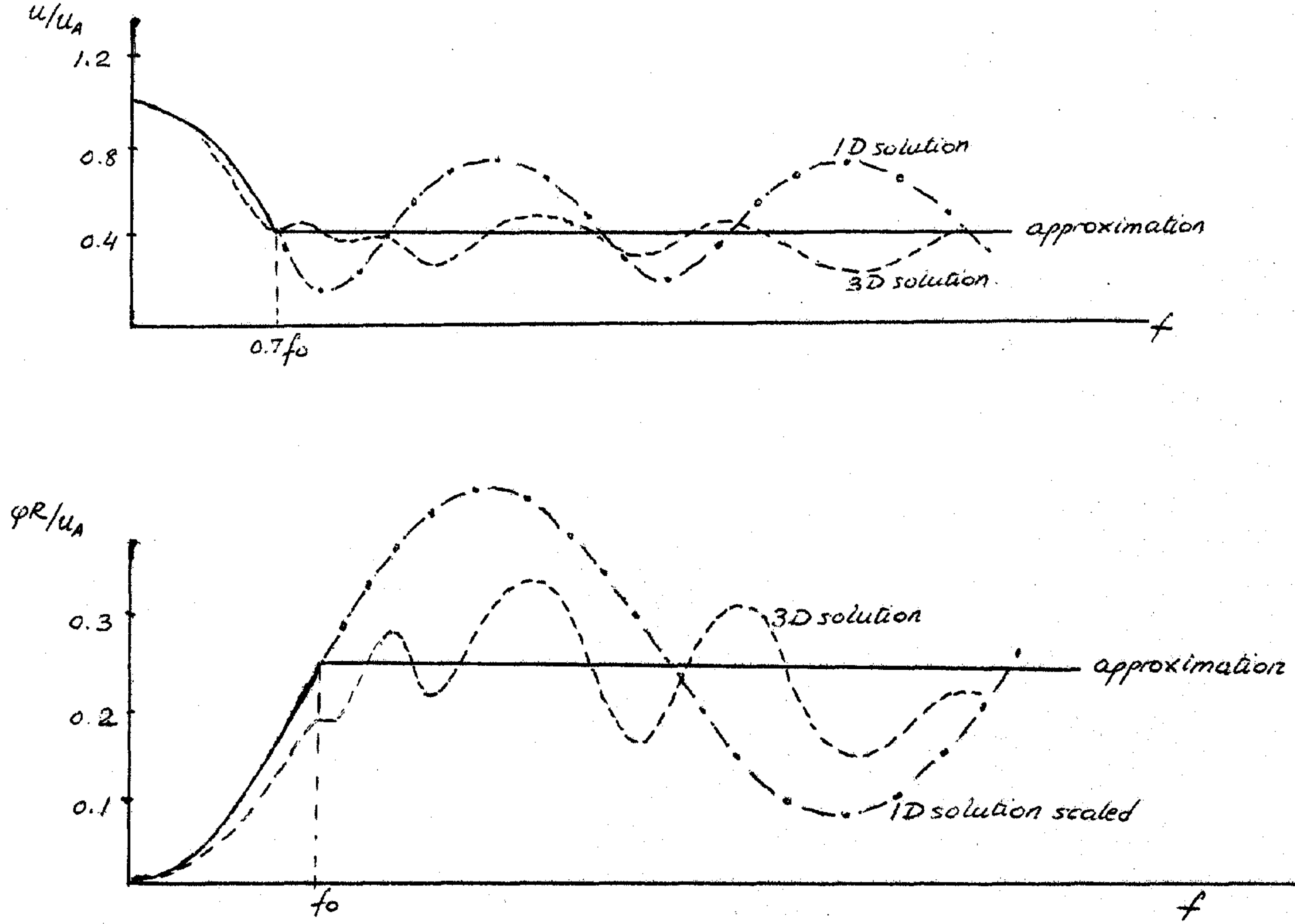

FIGURE 19 TRANSFER FUNCTIONS FOR VARIABLE SOIL PROFILE

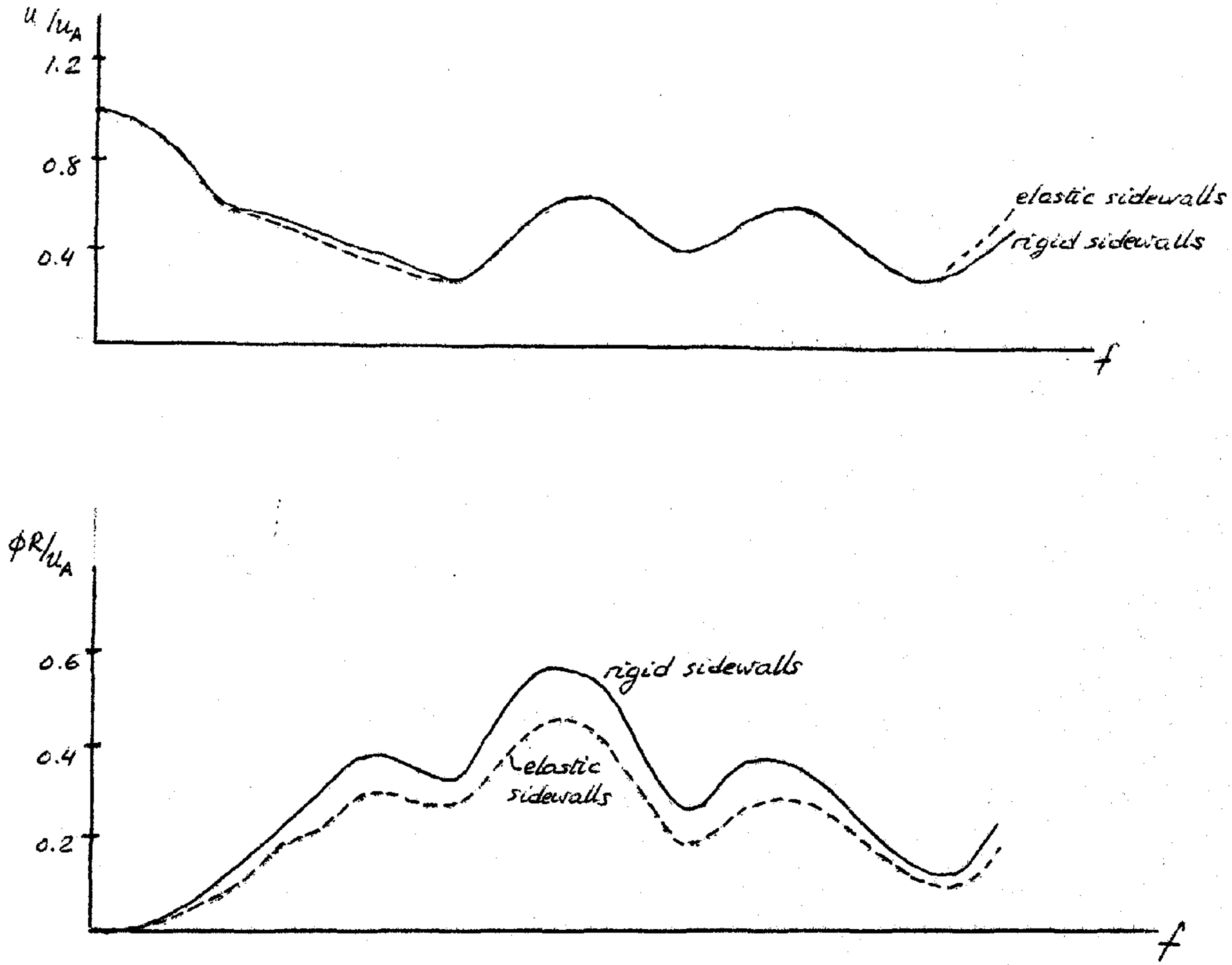

FIGURE 20 - EFFECT OF FLEXIBILITY OF SIDEWALLS ON TRANSFER FUNCTIONS

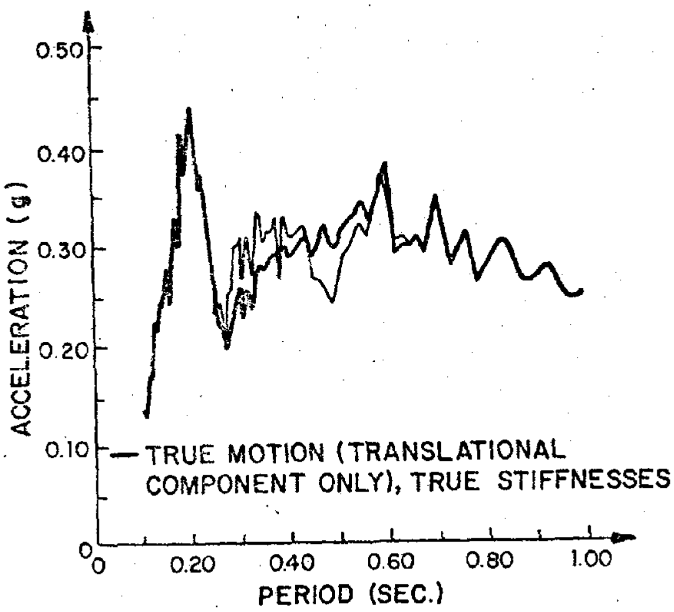

Foundation level

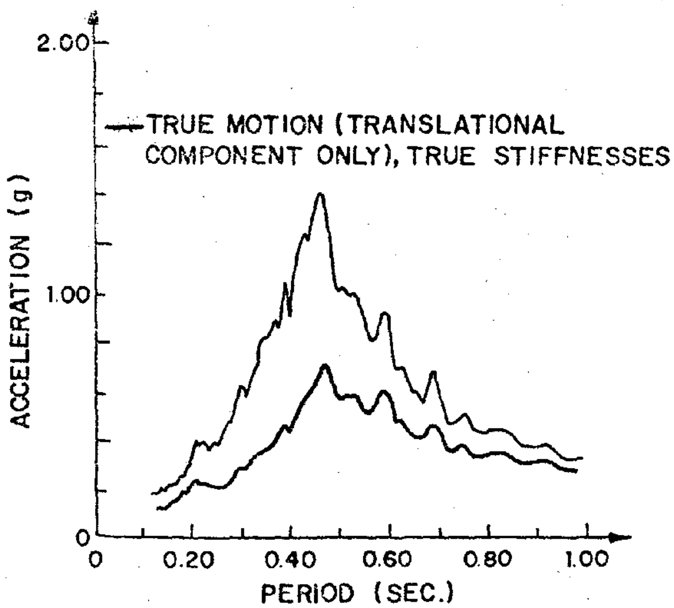

Top of Structure.

FIGURE 21 - EFFECT OF BASE ROTATION ON AMPLIFIED RESPONSE SPECTRA.

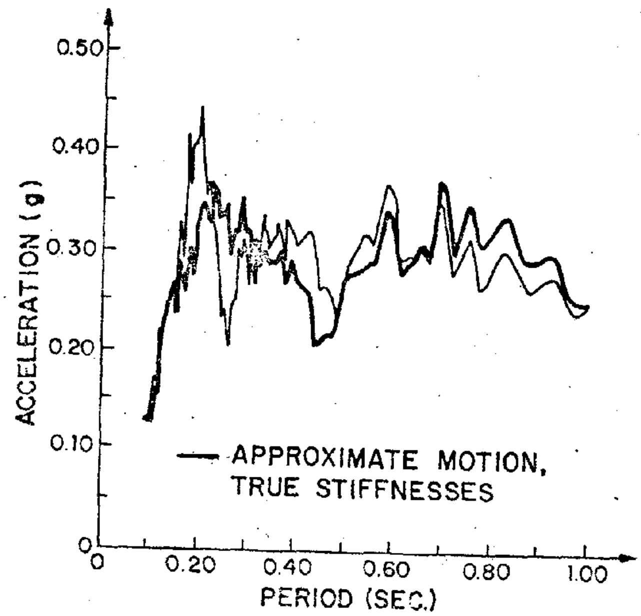

Foundation Level

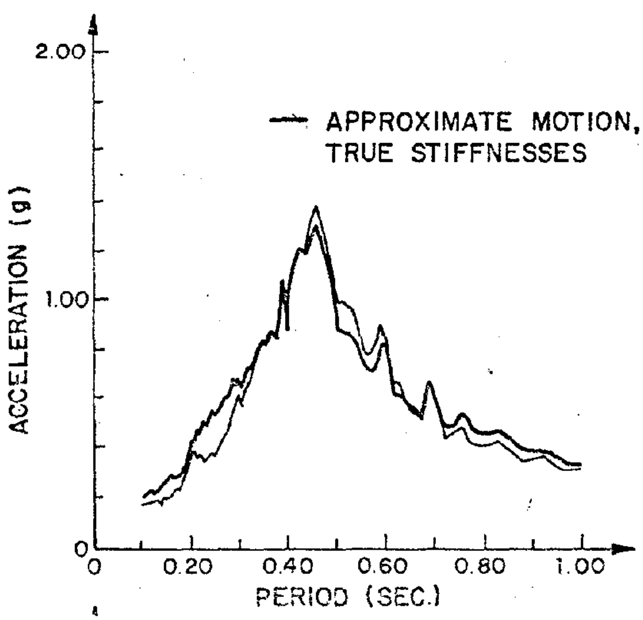

Top of Structure

FIGURE 22. Effect of approximate rules for motion on Amplified Response Spectra.

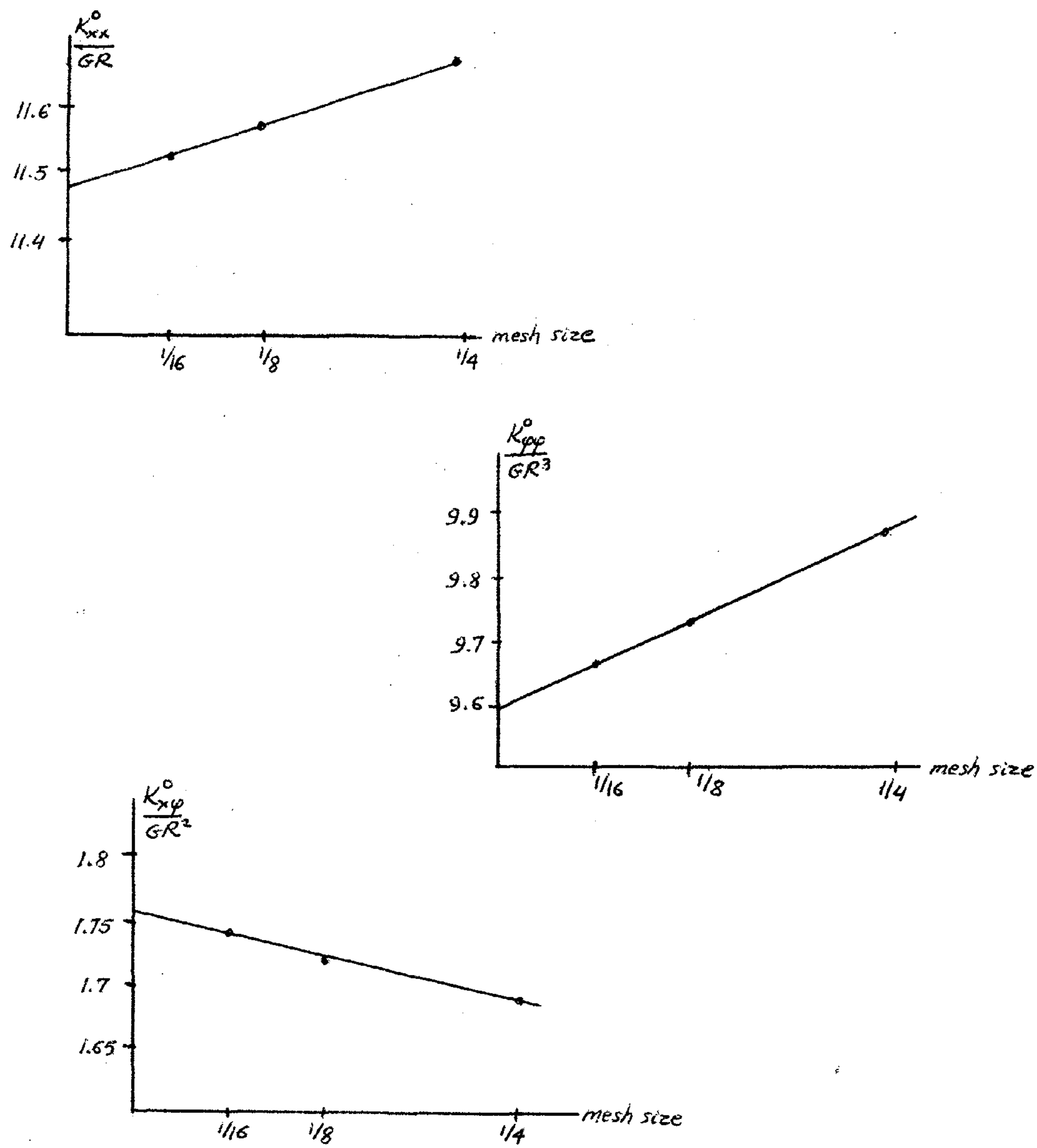

FIGURE 23. Extrapolation procedure for mesh size.

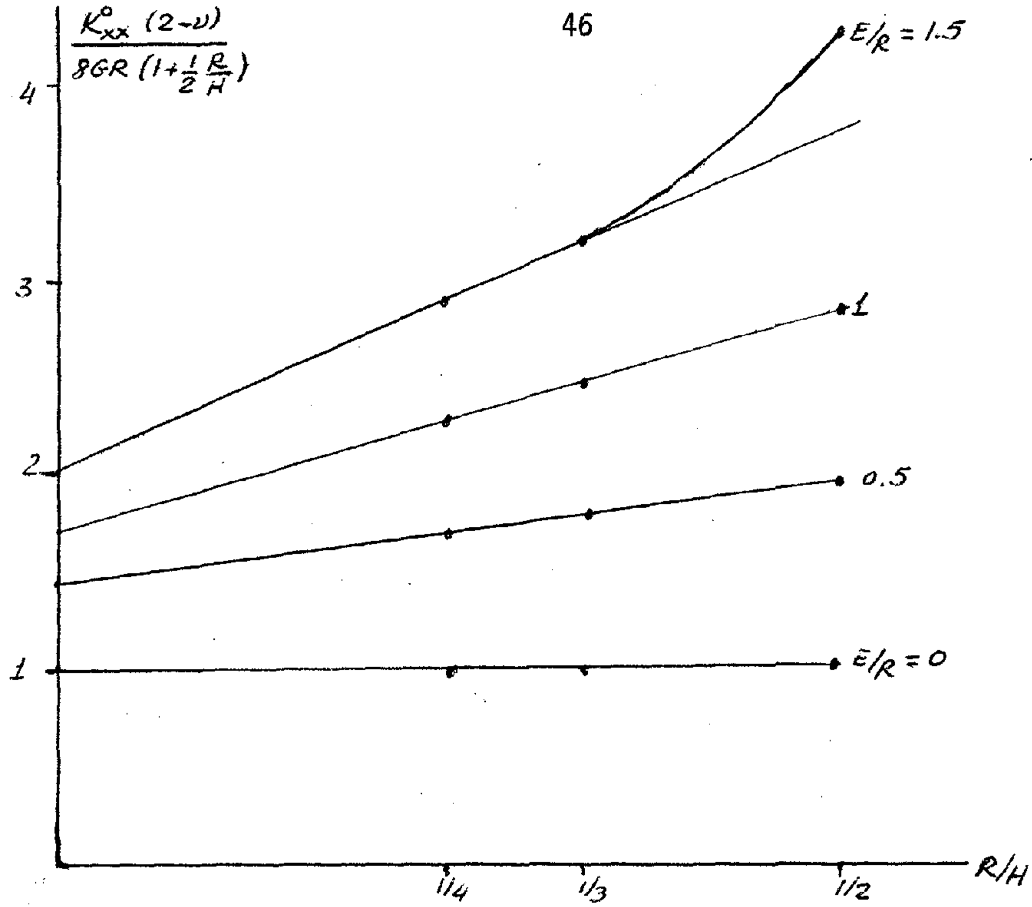

FIGURE 24. Variation of K^o_{xx} with R/H and E/R

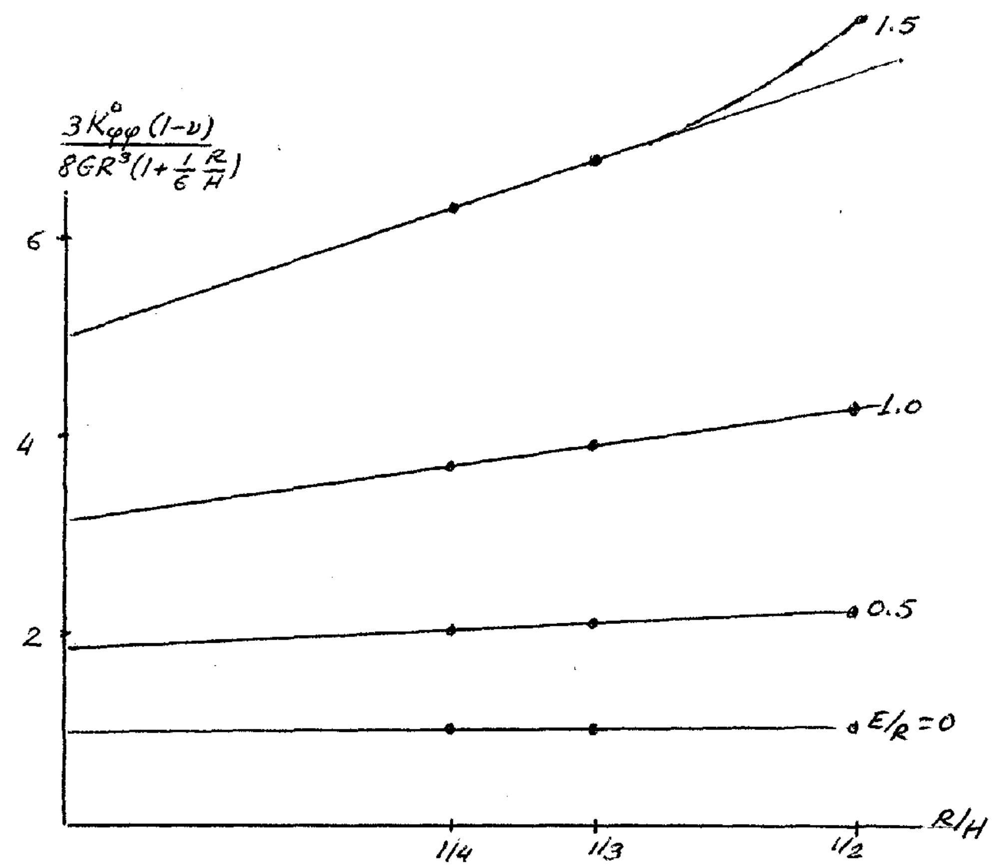

FIGURE 25. Variation of $K^o_{\varphi\varphi}$ with R/H and E/R.

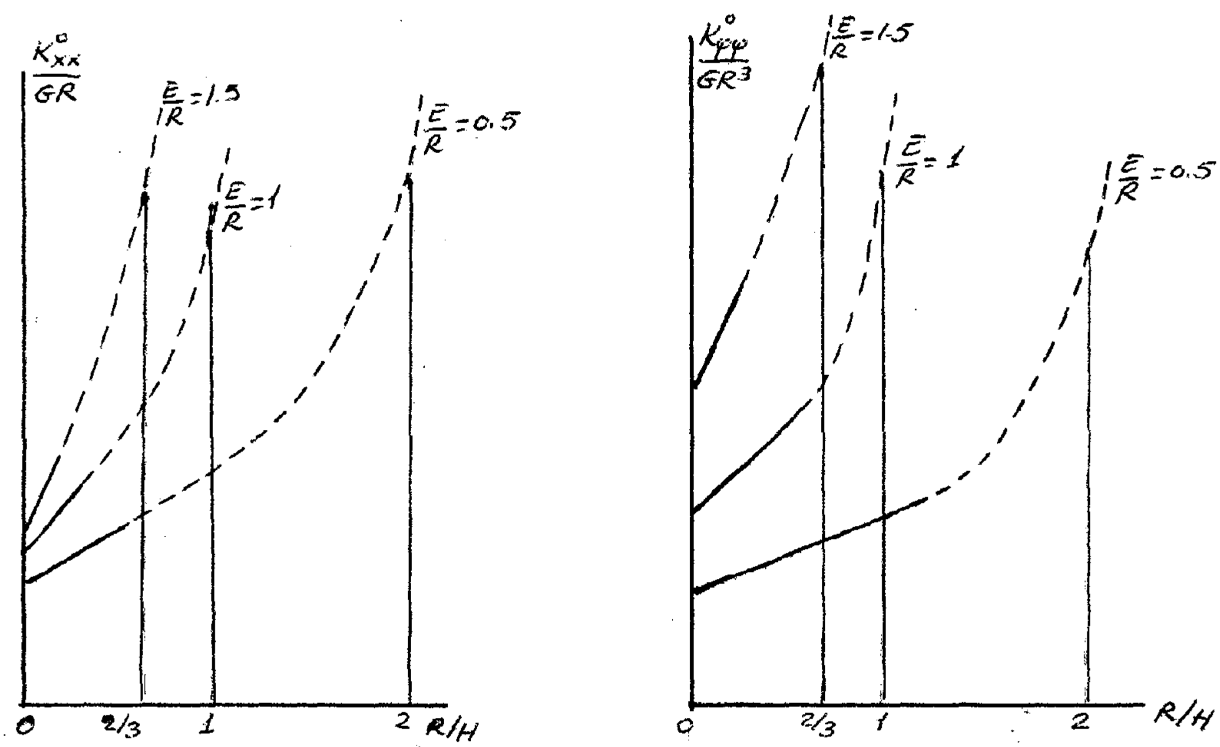

FIGURE 26. Schematic Variation of Stiffness Coefficients vs R/H.

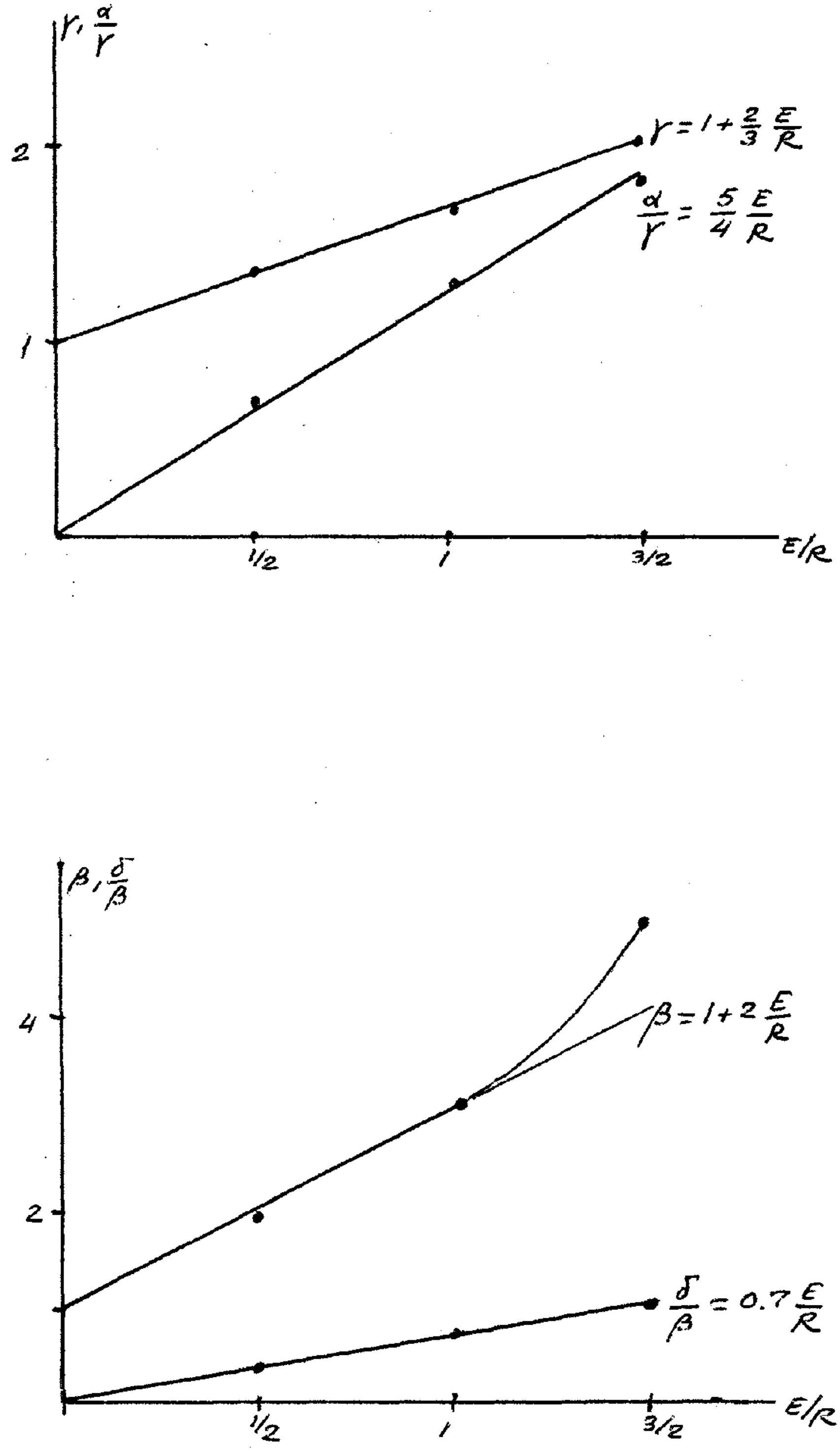

FIGURE 27 Determination of coefficients $\frac{\alpha}{\gamma}, \gamma, \frac{\delta}{\beta}, \beta$

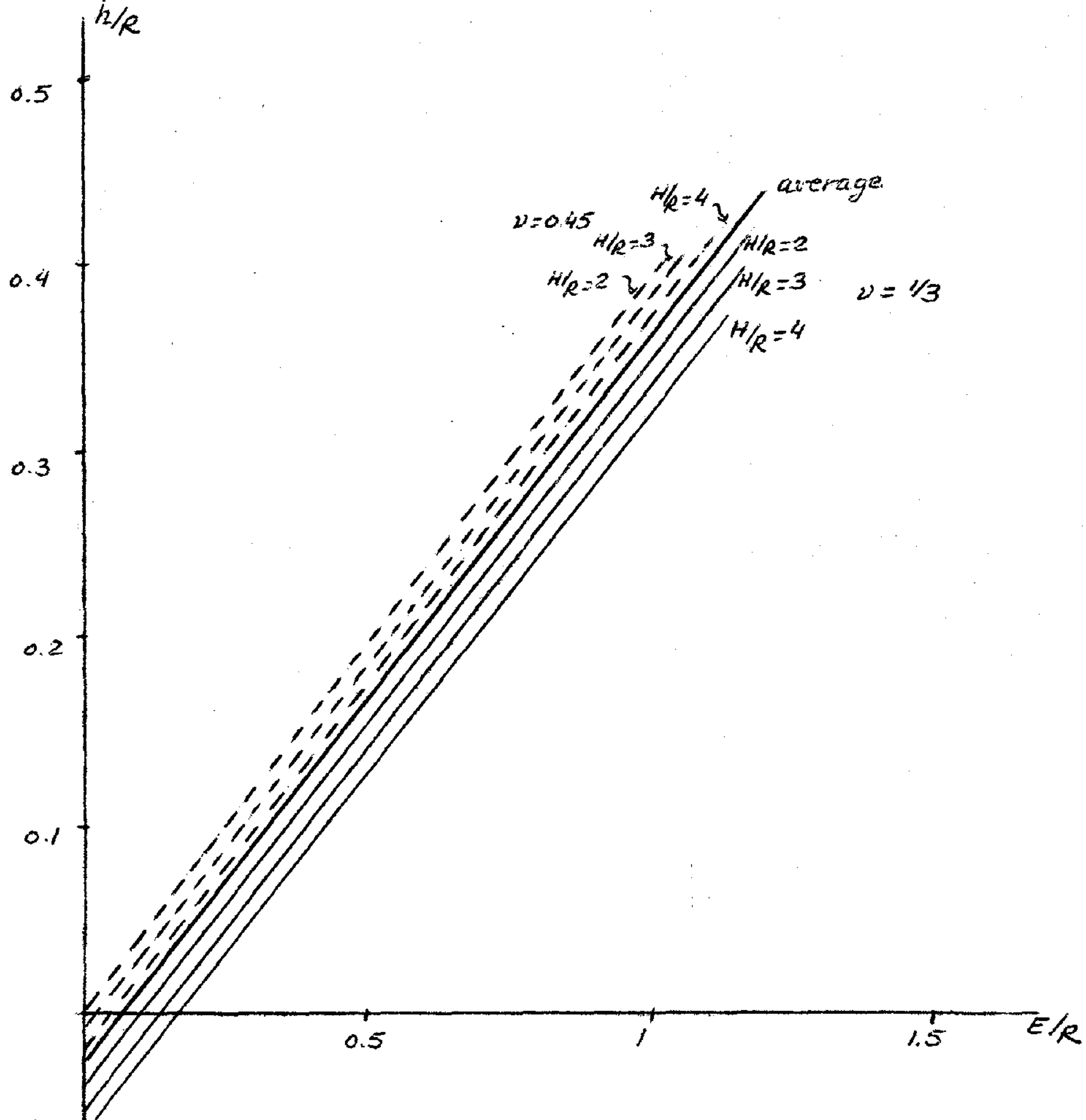

FIGURE 28 Variation of height of center of stiffness

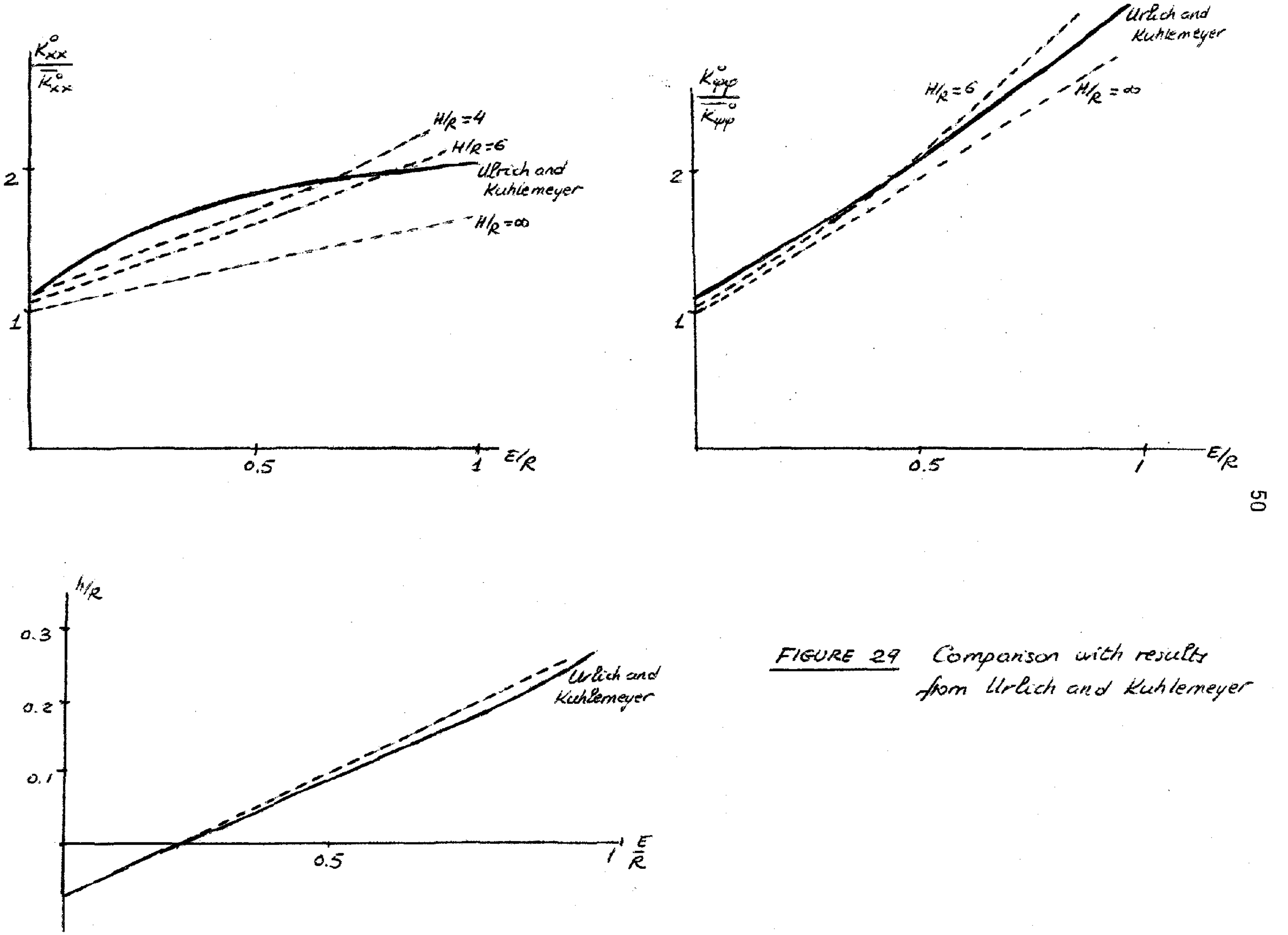

FIGURE 29 Comparison with results from Ulrich and Kuhlemeyer

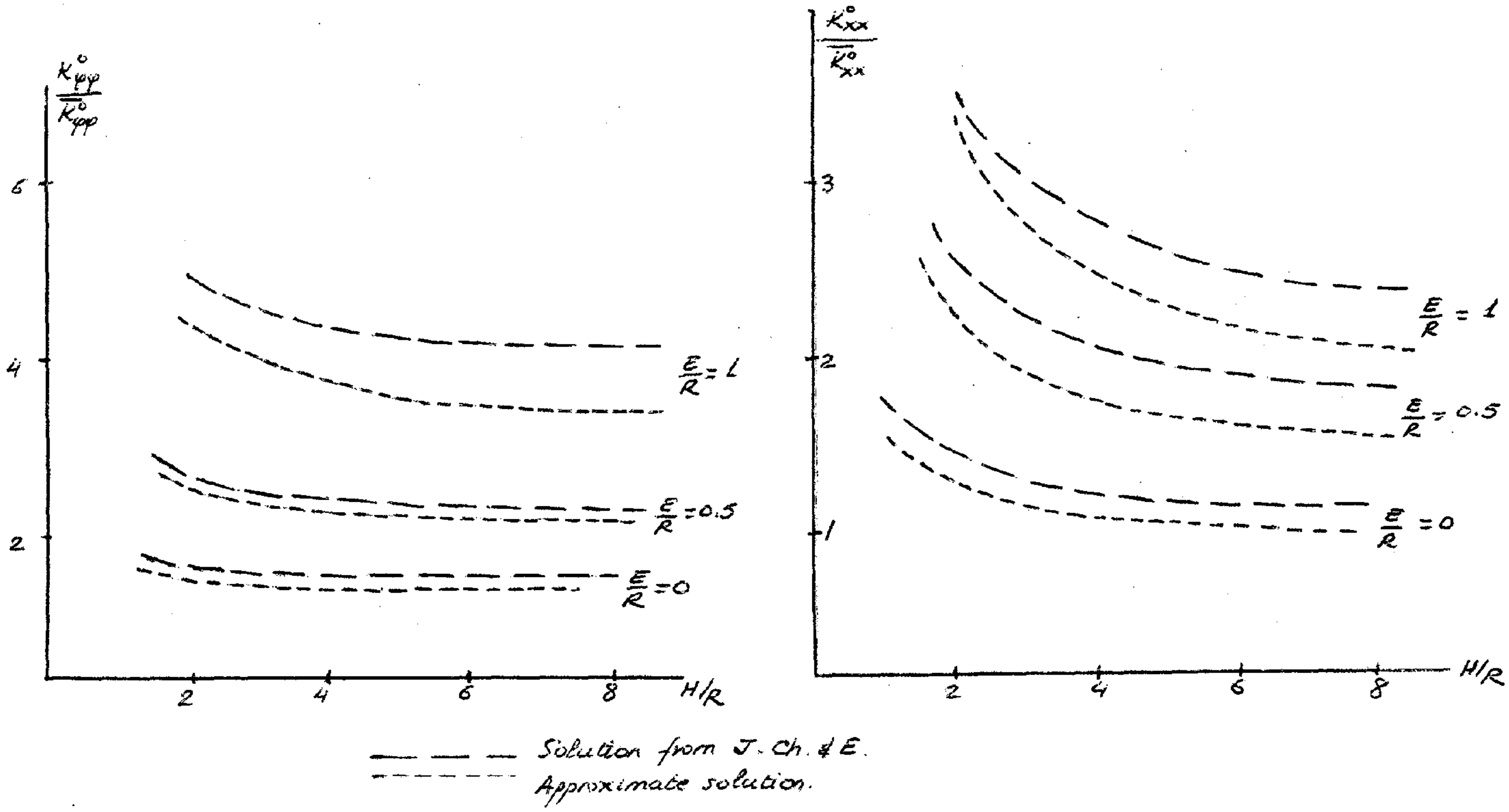

FIGURE 30 Comparison with results from Johnson, Christiano & Epstein.

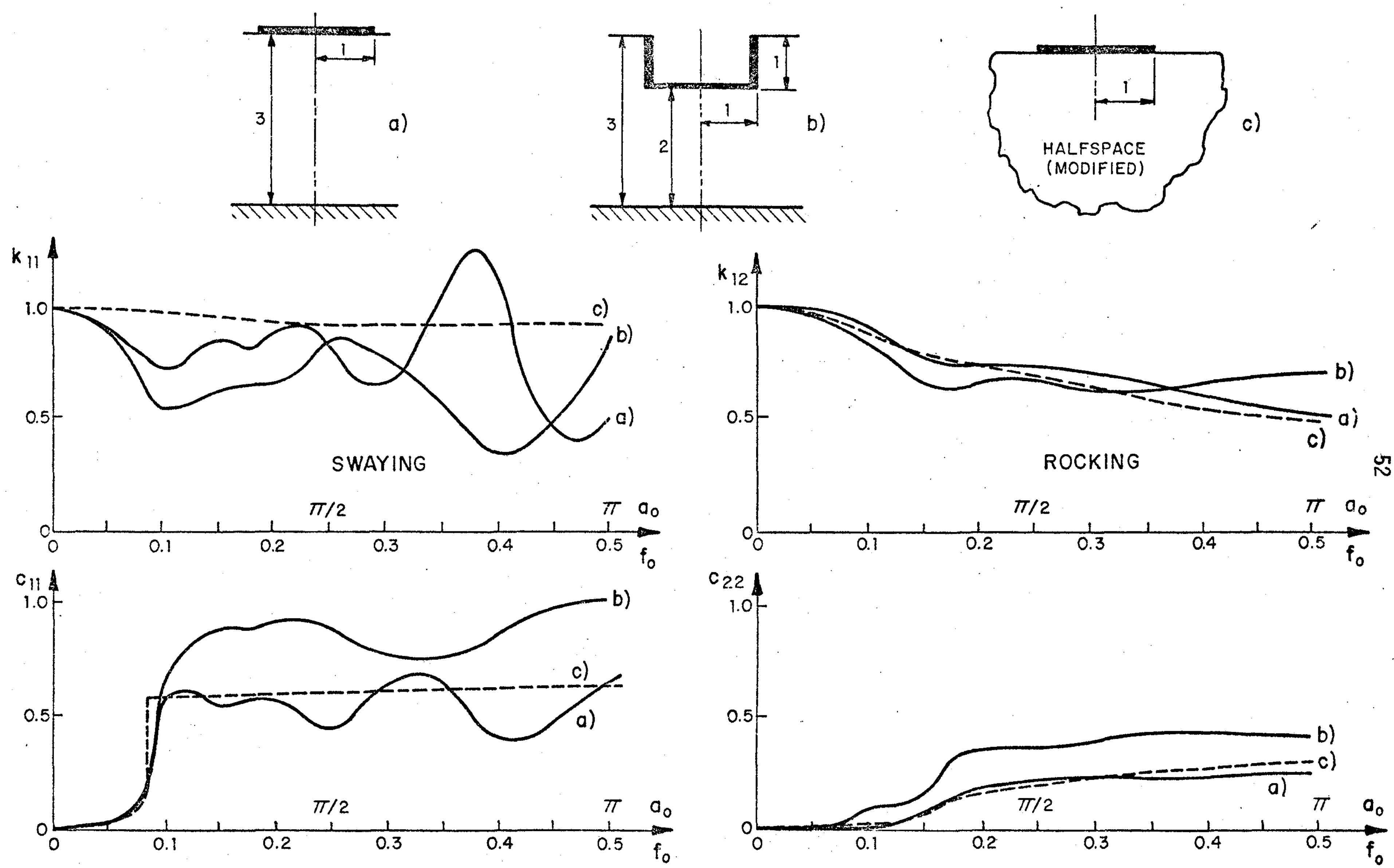

FIGURE 31

DYNAMIC STIFFNESS COEFFICIENTS, $\nu = 1/3$, $\beta = 0.05$

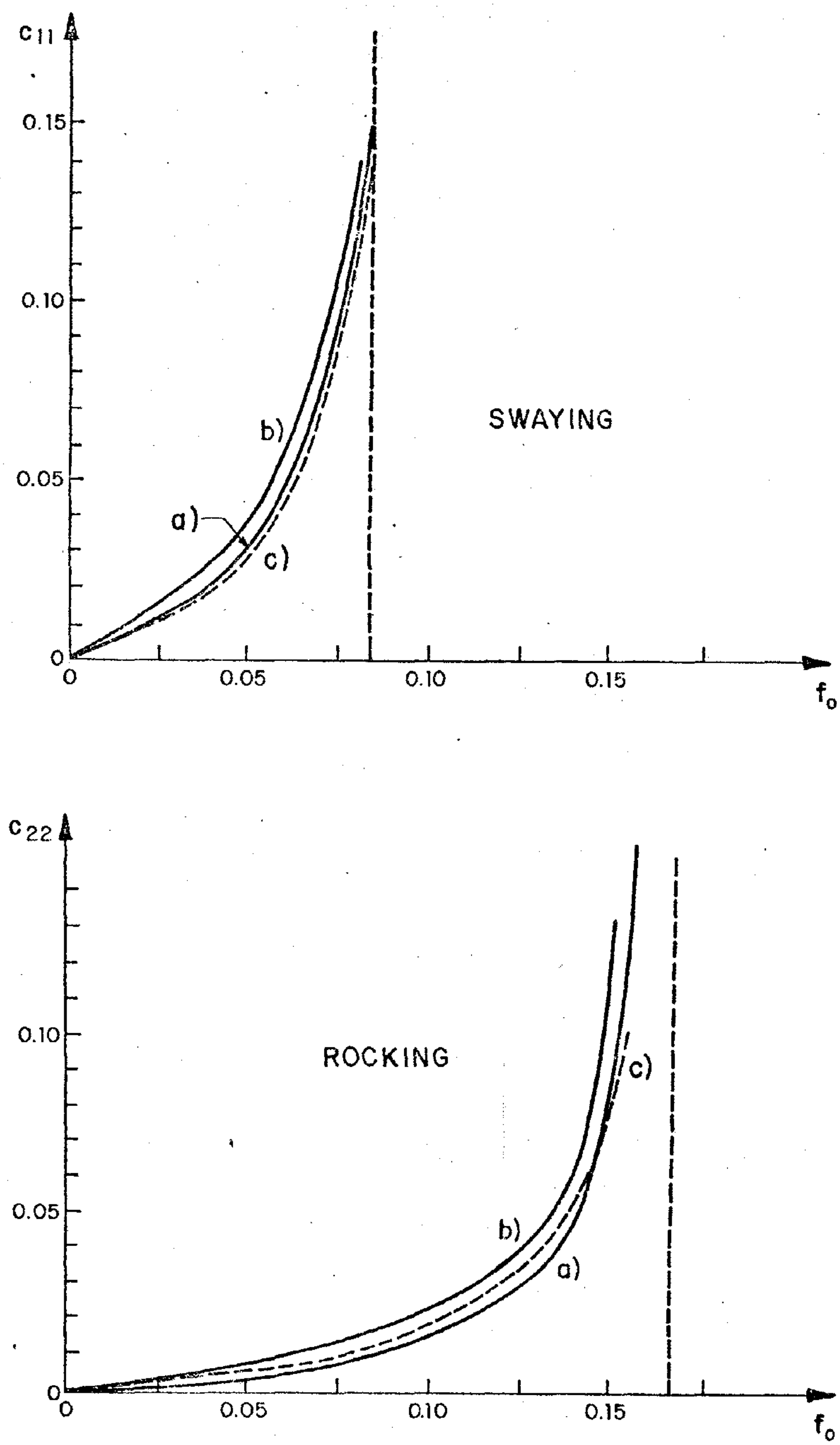

FIGURE 32

CLOSEUP OF DAMPING COEFFICIENTS IN LOW FREQUENCY RANGE; GEOMETRY AS SHOWN IN FIGURE 31

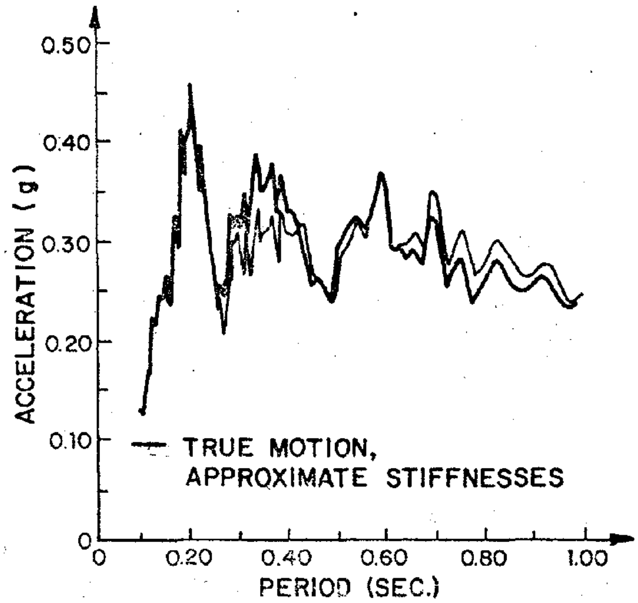

Foundation Level.

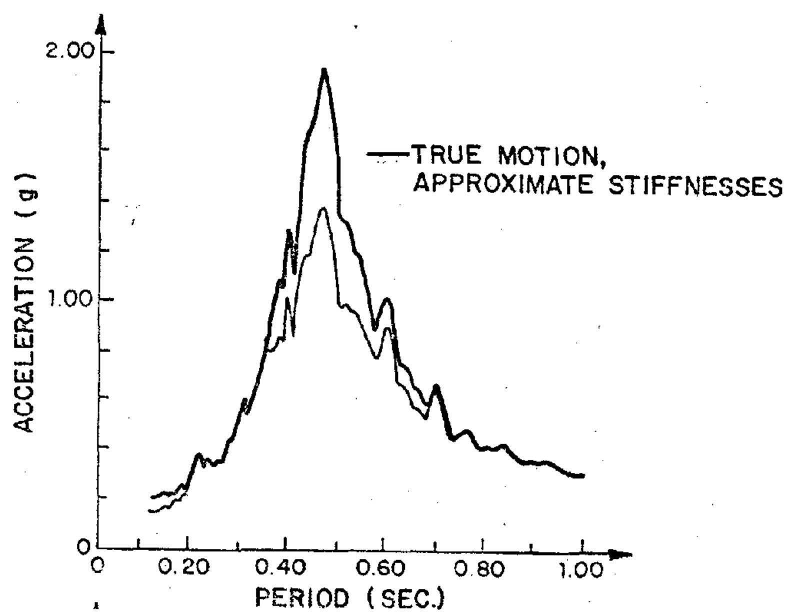

Top of Structure

FIGURE 33 - Effect of approximate stiffnesses on Amplified Response Spectra

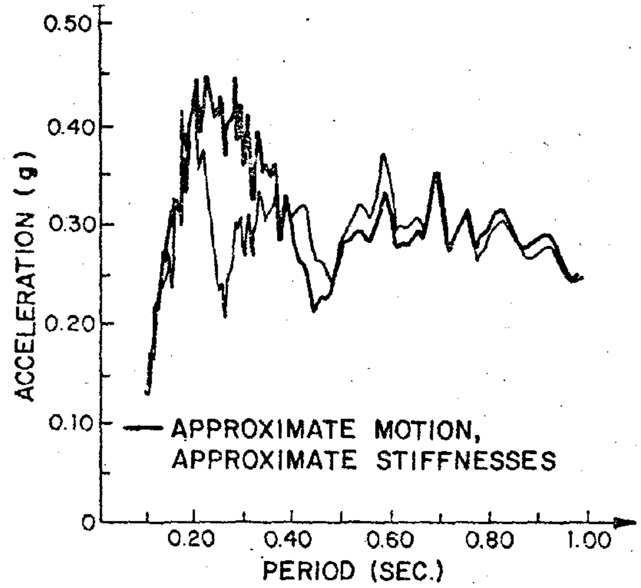

Foundation Level

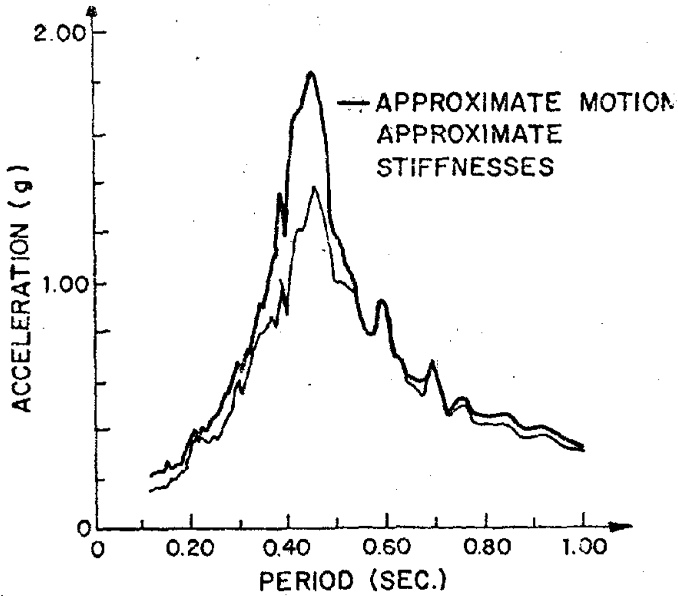

Top of Structure

FIGURE 34. Effect of approximate motions and stiffnesses on Amplified Response Spectra.